
Article:
Lanzoni, Lucilla, Ravasio, Daniela, Thompson, Hannah Elizabeth et al. (4 more authors) (2020) The role of default mode network in semantic cue integration. Neuroimage. 117019. ISSN: 1053-8119

https://doi.org/10.1016/j.neuroimage.2020.117019

The role of default mode network in semantic cue integration

Lucilla Lanzoni[1], Daniela Ravasio[2], Hannah Thompson[3], Deniz Vatansever[4], Daniel Margulies[5], Jonathan Smallwood[1] & Elizabeth Jefferies[1]

1 Department of Psychology, University of York, UK

2 Department of Psychological Sciences, University of Bergamo, Italy

3 School of Psychology, University of Surrey, UK

4 Institute of Science and Technology for Brain-inspired Intelligence, Fudan University, Shanghai, PR China.

5 Institute du Cerveau et de la Moelle épiniére (ICM), Paris, France

* Corresponding author1: Lucilla Lanzoni

Email: lucilla.lanzoni@york.ac.uk

Phone: 01904 322928

University of York, Heslington, York

YO10 5DD

* Corresponding author2: Elizabeth Jefferies

Email: beth.jefferies@york.ac.uk

Phone: 01904 324368

University of York, Heslington, York

YO10 5DD

UK

Funding

The study was supported by a grant from the Stroke Association [R1425201] and a grant from the European Research Council [FLEXSEM – 771863] awarded to E.J.

Declarations of interest: none

ABSTRACT

Recent accounts of large-scale cortical organisation suggest that the default mode network (DMN) is positioned at the top of a principal gradient, reflecting the separation between heteromodal and unimodal sensory-motor regions in patterns of connectivity and in geodesic distance along the cortical surface (Margulies et al., 2016). This isolation of DMN from external inputs might allow the integration of disparate sources of information that can constrain subsequent cognition. We tested this hypothesis by manipulating the degree to which semantic decisions for ambiguous words (e.g. JAM) were constrained by preceding visual cues depicting relevant spatial contexts (e.g. SUPERMARKET or ROAD) and/or facial emotions (e.g. HAPPY vs. FRUSTRATED). We contrasted (i) the effects of a single preceding cue with a no-cue condition employing scrambled images, and (ii) convergent spatial and emotion cues with single cues. Single cues elicited stronger activation in the multiple demand network relative to no cues, consistent with the requirement to maintain information in working memory. The availability of two convergent cues elicited stronger activation within DMN regions (bilateral angular gyrus, middle temporal gyrus, medial prefrontal cortex, and posterior cingulate), even though behavioural performance was unchanged by cueing – consequently task difficulty is unlikely to account for the observed differences in brain activation. A regions-of-interest analysis along the unimodal-to-heteromodal principal gradient revealed maximal activation for the convergent cue condition at the heteromodal end, corresponding to the DMN. Our findings are consistent with the view that regions of DMN support states of information integration that constrain ongoing cognition and provide a framework for understanding the location of these effects at the heteromodal end of the principal gradient.

Keywords: default mode, integration, principal gradient, semantics, cueing

1. INTRODUCTION

The context in which we encounter concepts in our daily life influences the manner in which we think about them. Hearing the word *jam* at the kitchen table, for example, one might activate a number of concepts related to food, its taste and emotional valence. The same word *jam* on the traffic news, however, might bring up very different thoughts and emotions. Although studies have manipulated sentence contexts to constrain the interpretation of ambiguous words (e.g. Noonan et al., 2010; Rodd et al., 2016; Rodd et al., 2005; Rodd et al., 2004; Rodd et al., 2013; Vitello & Rodd, 2015), cues beyond language have rarely been employed (for an exception see Lanzoni et al., 2019). Consequently, relatively little is known about how non-verbal cues, such as spatial location and affect, constrain meaning retrieval or the neural mechanisms that underlie this effect. The current study addressed this issue by manipulating the availability of spatial and facial emotion cues prior to semantic decisions about ambiguous words.

Contemporary models of semantic cognition suggest that retrieval is supported by a dynamic interplay of conceptual knowledge with retrieval processes (Hoffman et al., 2018; Jefferies, 2013; Lambon Ralph et al., 2016). Conceptual representations are rich and comprise features from multiple sensory modalities (e.g. an apple is a *sweet* fruit, with a *rounded* shape and a *smooth hard* surface which is often *red*, *yellow* or *green*). According to the Hub and Spoke model of conceptual representation, the ventrolateral anterior temporal lobe (ATL) 'hub' integrates features encoded in sensory-motor cortical 'spokes' to generate coherent representations – e.g. our concept 'apple' (Chiou & Lambon Ralph, 2019; Patterson et al., 2007; Lambon Ralph et al., 2016). However, hub and spoke representations are not sufficient to support *flexible* semantic cognition; we also dynamically vary the aspects of knowledge that we retrieve about concepts depending on the context. Semantic processing may draw on different large-scale networks depending on whether retrieval is usefully constrained or miscued by the context.

In line with this view, semantic sites have been shown to overlap with distinct large-scale networks that are recruited differentially depending on the task demands. When non-dominant associations are required by a task, or the prior context is unhelpful, a 'semantic control network' is recruited (including left inferior frontal gyrus and posterior middle temporal gyrus), which may shape retrieval to suit the circumstances (Badre & Wagner, 2005, 2006;

Davey et al., 2016; Hallam et al., 2016; Krieger-Redwood et al., 2015; Noonan et al., 2013; Whitney et al., 2011). In contrast, other key sites for semantic cognition, such as lateral ATL and angular gyrus (AG), have patterns of intrinsic connectivity that are partially overlapping with aspects of the Default Mode Network (DMN) (Davey et al., 2016; Humphreys & Lambon Ralph, 2014; Jackson et al., 2016; Seghier et al., 2010). The role of DMN regions in semantic cognition remains controversial: a meta-analysis by Binder and colleagues (2009) found peak activation for semantic tasks in AG, while other researchers have characterized AG as a task-negative region which deactivates across semantic and non-semantic tasks (Humphreys et al., 2015; Humphreys & Lambon Ralph, 2014; Mollo et al., 2017). DMN regions, including AG, typically show anti-correlation with task-positive regions within the multiple demand network (MDN; Blank et al., 2014; Davey et al., 2016; Fox et al., 2005). Nevertheless, TMS studies have shown that AG plays a critical role in the efficient retrieval of dominant aspects of knowledge (Davey et al., 2015). There are also demonstrations of a role for the DMN in semantic retrieval even when tasks are relatively hard. For example, Murphy et al. (2018) found greater DMN recruitment both when participants made judgements based on their memory of preceding trials (as opposed to stimuli present on the screen), and when the decisions involved semantic categories as opposed to perceptual features.

Recent studies have suggested that semantic regions allied to DMN, including AG, support the combination of concepts into meaningful and more complex representations (e.g. Price et al., 2015; for a review see Pylkkänen, 2019). These regions show a stronger response when coherent conceptual combinations or heteromodal features are presented (Bemis & Pylkkänen, 2011; Price et al., 2015; 2016; Pylkkänen, 2019; Teige et al., 2018; 2019). The suggested critical role of the DMN in conceptual integration fits well with the observation that the DMN lies at the top of a cortical hierarchy. Through decomposition of resting-state connectivity, Margulies et al. (2016) identified a principal gradient of macroscale organization, anchored at one end by sensory regions and at the other end by heteromodal cortex, corresponding to the DMN. This separation of DMN from unimodal cortex in intrinsic connectivity relates to geodesic distance – DMN sites are located relatively far away from primary sensory-motor cortex along the cortical surface (Margulies et al., 2016). Greater distance along the gradient might allow the brain to support forms of cognition that rely on memory, as opposed to information in the external environment (Murphy et al., 2019).

Distance might also support increasing levels of abstraction from sensory-motor features, allowing the formation of heteromodal conceptual representations from the integration of these diverse sources of information (Buckner & Krienen, 2013; Mesulam, 1998; Patterson et al., 2007; Smallwood, 2013). In line with this idea, default mode regions might show a greater response in semantic tasks when multiple aspects of a concept are activated during retrieval.

In the present study, we tested the view that semantically-relevant regions within the DMN, in particular AG, contribute to conceptual integration. We adopted a paradigm recently developed to assess the impact of non-verbal cues in patients with semantic aphasia, who have deficits of semantic control (Lanzoni et al., 2019). Participants were shown 0, 1 or 2 cues that were relevant to the subsequent interpretation of an ambiguous word: they saw photographs of spatial contexts, facial emotions or scrambled meaningless versions of these cues. The cues alone were not sufficient to prime the concepts and did not influence behavioural performance (for example, SUPERMARKET and HAPPY FACE can be linked in many ways and do not strongly anticipate JAM AS FOOD). Nevertheless, the cues allowed the subsequent semantic decisions to unfold in a conceptually-rich context. If semantic integration occurs in the DMN, comparing semantic decisions in the context of multiple convergent cues as opposed to single cues should reveal increased activation within this network and in particular in AG – even though semantic decisions to ambiguous words are relatively cognitively effortful. In contrast, brain regions that selectively encode and maintain semantic cue information *prior* to integration should be spatially distinct from DMN: the neural basis of cue maintenance might be maximally revealed by a contrast of single cue over no cue trials (as this contrasts situations where there are working memory demands versus no requirement to maintain information). MDN is a candidate network for attentional and working memory components of the cueing task, since this network is associated with executively demanding aspects of cognition, including working memory and the maintenance of task rules, across domains (e.g. Owen et al., 2005; Naghavi & Nyberg, 2005; Dosenbach et al., 2006). For example, a study by Dumontheil et al. (2010) found activation in several parts of MDN during the presentation of task instructions, which might reflect the creation of a task-model or framework for ongoing cognition.

Additionally, we predicted that the effect of conceptual integration but not cue load would be located at the heteromodal end of the principal gradient (Margulies et al., 2016), providing a framework for understanding *why* information integration effects occur where

they do within the cortex: these effects should be greatest at the DMN apex of the gradient, which is maximally separated (both in terms of physical distance and in connectivity terms) from unimodal input or 'spoke' regions associated with processing specific features. In contrast to our standard whole-brain cluster-corrected contrasts, the focus of this analysis was not on the functional contribution of specific regions, such as AG, to cue integration, but instead on whole-brain patterns that include similar functional transitions between heteromodal and unimodal cortex in distant cortical regions.

2. MATERIALS AND METHODS

2.1 Participants

Twenty-seven healthy right-handed native English-speaking participants with normal or corrected-to-normal vision were recruited from the University of York (9 males, mean age 21.5, SD 2.9, range 19-30). Participants received monetary compensation or course credits. One dataset was excluded due to technical problems that resulted in no behavioural responses being recorded, leaving 26 subjects in the final sample. In a subsequent analysis we examined resting-state fMRI data from 86 participants (22 males; mean age 20.3, range 18–32 years), twelve of whom were also in the main sample. The research was approved by the York Neuroimaging Centre Ethics Committee and participants provided written informed consent.

2.2 Materials

The cueing paradigm, adapted from Lanzoni et al. (2019), presented pictures of facial expressions and spatial locations prior to semantic judgements about ambiguous words. The stimuli are available on the Open Science Framework (https://osf.io/wp6a7/)[1]. Thirty English homonyms were selected from the Free Association Norms of Twilley et al. (1994), and the Gawlick-Grender & Woltz norms (1994). We chose items where the different interpretations were associated with different facial expressions (e.g. JAM with *traffic* is associated with frustration while JAM with *strawberry* is associated with pleasure). We also chose items where different interpretations were associated with different locations (e.g. a motorway for *traffic* JAM and a supermarket for *strawberry* JAM). We then generated four target words for each

[1] The images of spatial locations are not included in the collection due to potential copyright restrictions.

probe, two for each interpretation. This resulted in 120 probe-target pairs. For instance, the probe JAM appeared in four trials, twice paired with a target referring to *traffic* (JAM-horn or JAM-delay) and twice paired with a target referring to the alternative interpretation (JAM-spoon or JAM-bread). Although we did not manipulate the difference in frequency between the two alternative meanings, one interpretation of the homonym was dominant over the other (i.e., a larger proportion of subjects generated words linked to that interpretation, as reported in Twilley et al., 1994). Dominance was controlled by counterbalancing the assignment of each interpretation to the different experimental conditions across participants. For each combination of probes and targets, two unrelated distractors were selected. Latent Semantic Analysis (as implemented in lsa.colorado.edu) was used to calculate the similarity in semantic space between the probe and the targets vs. probe and distractors (parameters used: space – General reading up to 1st year college, comparison type - term to term, number of factors – maximum). This confirmed that the strength of the relationship between probe and distractor ($M = .08$, $SD = .04$) was significantly weaker compared to the association between probe and target ($M = .22$, $SD = .10$; $t(29) = 7.17$, $p < .001$). Distractors and target words were matched for lexical frequency (SUBTLEX-UK database, van Heuven et al., 2014; $t = .89$, $p = .380$), word length ($t = -1.44$, $p = .154$), and concreteness (Brysbaert et al., 2014; $t = .58$, $p = .564$).

Pictures of facial emotional expressions and spatial locations were used to prime the relevant meaning of the homonym. Each picture was used only once across the entire experiment, making it impossible for participants to predict the following probe word on the basis of the cue. Images of facial expressions were chosen from the Radboud Faces Database (Langner et al., 2010) and included eight basic emotions: happy, angry, sad, disgusted, contemptuous, surprised, neutral, fearful. In selecting the affect cues we ensured that the same face from the Radboud Database would not be presented in the same emotional expression in other trials. Therefore, for trials that required the same emotional expression we chose different actors. Pictures of spatial contexts were downloaded from Google images.

The emotion and location cues could appear together in the same trial (2 cues condition), they could be presented alone (1 cue affect or location conditions), in which case they were paired with one meaningless scrambled image, or two scrambled images were provided (no-cue condition). Images were converted to greyscale, matched for luminance and scrambled using the SHINE toolbox (Willenbockel et al., 2010). Images were also brought to a

fixed dimension (600 x 400 pixels for location and 260 x 400 for affect cues) using Matlab (The MathWorks Inc., Natick, MA, US). Figure 1B shows the 4 cue conditions, which were used to examine three levels of constraint on semantic retrieval. The location of the emotion and location cues (to the left or right of the screen) was counterbalanced within each run. Finally, to ensure that people could not make their decisions based only on the cue, in each trial one of the distractors was related to either the emotional cue or the visuo-spatial cue presented before the semantic task (in Figure 1A, the distractor 'bag' is related to the location cue – supermarket). The assignment of the emotion-related and location-related distractors to the different conditions was counterbalanced within participants, such that each probe appeared twice with an emotion-related distractor and twice with a location-related distractor.

2.3 Procedure

The MRI session included a high-resolution structural scan, a FLAIR sequence and four functional runs of approximately nine minutes each. Each trial started with a fixation cross of random duration between 1500 and 3000ms (Figure 1A). Two cue pictures or scrambled cues were then presented for 1s, followed by another jittered inter-stimulus interval (ISI: 1500 – 3000ms). Participants were asked to pay attention to the cues, and they were told that these would be helpful images on some trials, and meaningless images on other trials. Next, four words appeared on screen – a probe word at the top and three response options underneath, marking the start of the semantic task. Participants were asked to decide which of the three options had the strongest semantic relationship to the probe, and they were encouraged to make the semantic decision based on the words and not on the previously seen images. Although the time to respond was fixed (4s), participants were asked to respond as quickly and accurately as possible. Each of the 30 probes was presented once within each run, resulting in 30 semantic trials. The order of presentation was randomized and stimuli were counterbalanced so that, across all participants, each probe-target combination appeared in all four cue conditions. Each run had a total of eight non-semantic trials, in which words were replaced with strings of the letter 'X' matched in length to the words. Here the task was to press any key. The scrambled images used in non-semantic trials were created equally often from face and location photos. Two null trials were also included to improve task modelling. During null trials participants saw a blank screen for the same duration of 4 seconds.

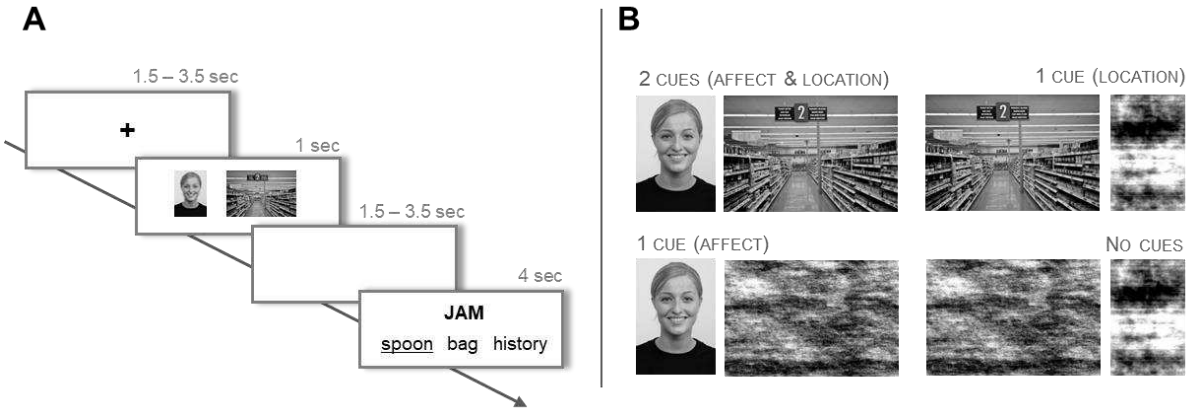

Figure 1. A. After an initial fixation cross (1500 – 3000 ms), participants were presented with cue images for 1000 ms, before moving to a blank screen (1500 – 3000 ms). Following that, a probe word was presented above a target and two unrelated distracters, triggering the onset of the decision-making period. The probe and choices remained visible for a fixed interval of 4000 ms. B. The four levels of the variable cue are shown.

2.4 fMRI acquisition

Whole brain fMRI data acquisition was performed using a GE 3 Tesla HDx Excite MRI scanner. Structural MRI data acquisition in all participants was based on a T1-weighted 3D fast spoiled gradient echo sequence (TR = 7.8ms, TE = minimum full, flip-angle = 20°, matrix size = 256x256, 176 slices, voxel size = 1.13×1.13×1 mm). A gradient-echo EPI sequence was used to collect functional data from 60 interleaved bottom-up axial slices aligned with the temporal lobe (TR = 3s, TE = 18.9 ms, FOV = 192x192x180 mm, matrix size = 64x64, slice thickness = 3mm, slice-gap = 3mm, voxel size = 3x3x3 mm^3, flip-angle = 90°). An intermediary FLAIR scan with the same orientation as the functional scans was collected to improve the co-registration between subject-specific structural and functional scans.

2.5 Data preprocessing

2.5.1 Behavioural pre-processing and analysis

We examined accuracy, median response time (RT), RT variability and response efficiency in separate repeated-measures ANOVAs to characterise differences in performance across the 4 semantic conditions (0 cues, 1 cue affect, 1 cue location, 2 cues: affect and location). One keypress was not recorded for two participants and these missing RT values were replaced with the group median for that condition. Response efficiency scores were used to account for any speed-accuracy trade-offs: the median RT for correct responses for each subject in each

condition was divided by the mean accuracy in the same condition (Townsend & Ashby, 1983). We also examined trial-to-trial variability, using the standard deviation of RT for each participant in each condition.

2.5.2 MRI data pre-processing

FMRI data processing was carried out using FEAT (FMRI Expert Analysis Tool) Version 6.0, part of FSL (FMRIB's Software Library, www.fmrib.ox.ac.uk/fsl). Registration of the high resolution structural to standard space (Montreal Neurological Institute – MNI) was carried out using FLIRT (Jenkinson et al., 2002; Jenkinson & Smith, 2001). Pre-processing of the functional image included motion correction using MCFLIRT (Jenkinson et al., 2002), slice-timing correction using Fourier-space time-series phase-shifting (interleaved), non-brain removal using BET (Smith, 2002), spatial smoothing using a Gaussian kernel of FWHM 5mm, grand-mean intensity normalisation of the entire 4D dataset by a single multiplicative factor, and high-pass temporal filtering (Gaussian-weighted least-squares straight line fitting, with sigma=50.0s).

2.6 Statistical modelling

Pre-processed time series were modelled using a general linear model using FILM correcting for local autocorrelation (Woolrich et al., 2001). We used an event-related design. We built two separate models, a *semantic decision model* to look for brain changes during semantic decisions following different levels of cueing, and a *cue model* to identify brain regions that responded to the presentation of the cues. Our key focus was on the semantic decision model, since this established whether specific networks or gradient patterns were associated with making semantic decisions in the context of single or convergent cues. The *semantic decision model* included 8 EVs: correct semantic decisions following each of the 4 experimental conditions (0 cues, 1 cue affect, 1 cue location, 2 cues), non-semantic trials where strings of "Xs" were presented, remaining time in the semantic trials after making a decision before the start of a new trial, cue presentation period (combining all the cue presentation events, irrespective of the cue condition), and incorrect semantic trials. Given that this model revealed two distinct networks associated with the maintenance of single cues as opposed to no cues, and the convergence of multiple cues vs. a single cue, we then elected to examine the response during cue presentation in a second stage of the analysis. The *cue model* included 6 Explanatory Variables (EVs) corresponding to the 4 cue conditions (0 cue condition containing scrambled

images, 1 face cue + scrambled image, 1 location cue + scrambled image, 2 cues: face and location), the semantic task, and the non-semantic task. The cue model established whether MDN regions responding to one > no cues showed load-dependent effects during cue encoding, consistent with increasing working memory demands of cue maintenance. However, it is important to acknowledge that the study was not designed to examine the cue phase in this fashion, and there are limitations of this exploratory analysis – in particular, the study did not de-confound the order of the cue presentation and semantic decision phases, as cues were always followed by the semantic task (albeit separated by a jittered interval; see limitations in Discussion). All regressors were modelled using a variable epoch model, with the appearance of the words (or the cue images, for the *cue model*) as the start of the event and the response time (or the duration of the cue presentation) as the duration of the event. Convolution of the hemodynamic response was achieved using a Gamma function (phase = 0, SD = 3, mean = 6). Temporal derivatives were added to each regressor. Nuisance regressors included standard + extended motion parameters. Absolute framewise displacement ranged from 0.05 mm to 0.64, with a mean value of 0.21 mm across the 4 runs.

We then averaged contrast estimates over the four runs within each subject using a fixed effects model, by forcing the random effects variance to zero in FLAME (FMRIB's Local Analysis of Mixed Effects) (Beckmann et al., 2003; Woolrich, 2008; Woolrich et al., 2004). The group analysis was carried out using FLAME (FMRIB's Local Analysis of Mixed Effects) stage 1 (Beckmann et al., 2003; Woolrich, 2008; Woolrich et al., 2004). Z (Gaussianised T/F) statistic images were thresholded using clusters determined by $z > 3.1$ and a (corrected) cluster significance threshold of $p = 0.05$ (Worsley, 2001). Our analysis focused on the comparison between semantic decisions which followed different levels of cue: 2 cues > 1 cue (collapsing across emotion and location cues) and 1 cue > 0 cues.

Cognitive decoding of the main contrasts of interest was performed in Neurosynth, an automated meta-analysis tool (Yarkoni et al., 2011). Unthresholded z maps were uploaded to Neurosynth to obtain psychological terms associated with the patterns of activation in our results. Where multiple terms had the same meaning (e.g. default, default mode, DMN, network DMN, default network), only the word with the highest correlation value was retained. This analysis provides additional evidence about the functional role of the regions within

different maps, by comparing the results to previous studies which have reported similar patterns of activation.

Finally, we wanted to examine whether the observed pattern of BOLD response in DMN regions reflected the macroscale cortical organization captured by the principal gradient (Margulies et al., 2016). In line with previous studies by our group (Murphy et al., 2018, 2019), this analysis leverages the explanatory power of the unimodal to heteromodal gradient to account for differences between experimental conditions. Consistently with our predictions of greater DMN recruitment during information integration, we expected to observe a higher response in regions towards the heteromodal end of the gradient in the 2>1 contrast. Decile bins along the gradient were calculated using the methods outlined by Margulies et al. (2016). The original gradient map provided values from 0 to 100 for each voxel in the brain (0 = unimodal end; 100 = DMN). This map was then divided into ten-percentile bins: all voxels with values 0–10 were assigned to bin1; voxels with values 11–20 to bin 2, etc., yielding 10 bins in total. The total number of voxels in each bin was near-identical (each contained 6133 to 6135 voxels). This analysis provides unique insights by focusing on whole-brain patterns associated with particular aspects of cued semantic retrieval, as opposed to the role of specific brain regions. The analysis can establish whether peaks associated with cue integration across the cortex are located at the apex of the gradient from heteromodal to unimodal processing, in line with the expectation that heteromodal cortex supports information convergence.

3. RESULTS

3.1 Behavioural results

A repeated measures ANOVA examining response efficiency revealed no significant differences across conditions [$F(3,75) = .62$, $p = .605$, $\eta^2 = .02$], indicating that semantic decisions following two cues were not easier than trials with less contextual support (one cue or no cue). The means and standard error for each condition are provided in Figure S1 and Table S1 (Supplementary Materials). There were also no significant differences between conditions in accuracy [$F(3,75) = .14$, $p = .939$, $\eta^2 = .01$], median response time [$F(3,75) = .95$, $p = .420$, $\eta^2 = .04$] or response time variability [$F(3,75) = 1.26$, $p = .296$, $\eta^2 = .05$]. All statistical values are provided in Table S2.

3.2 fMRI results

First, we report the whole-brain univariate results for models examining (i) how the BOLD response during semantic decision-making changes as a consequence of cues (semantic decision model) and (ii) the response to cue presentation (cue model). The coordinates for cluster peaks are reported in Table S3 (Supplementary Materials) and statistical maps are available in Neurovault (https://neurovault.org/collections/6198/). Next, to test one account of the response to single cues vs. no cues during semantic decision-making, we present a region of interest (ROI) analysis examining the response to different numbers of cues during cue presentation, in regions defined by the semantic decision model. This exploratory analysis establishes whether these regions behave in a load-dependent manner during cue encoding. Finally, we examine whether integration effects in DMN regions are captured by a macroscale gradient of cortical organization, using a series of ROIs positioned from the heteromodal to the unimodal end of this gradient. Figures were created using BrainNet Viewer (Xia et a., 2013; http://www.nitrc.org/projects/bnv/) and Surf Ice (https://www.nitrc.org/projects/surfice/).

3.2.1 Whole-brain results

Semantic decision model

Figure 2A shows the contrast between uncued semantic decisions and responses to letter strings (also uncued), while Figure 3 shows the response to different cue contrasts (1 cue vs. 0 cues; 2 cues vs. 1 cue). The supplementary materials provide contrasts between semantic and letter string trials for each of the cue conditions separately (Figure S3). These maps show a similar semantic response across conditions, which resembles the contrast of 0 cues over letter strings.

The contrast between semantic decisions without cues and non-semantic trials revealed activation in brain areas previously associated with semantic cognition (in studies that largely did not employ cues; e.g. Binder et al., 2009; Noonan et al., 2013; Seghier et al., 2004; Bright et al., 2004; Gold et al., 2005; Chee et al., 2000; for reviews see Lambon Ralph et al., 2016; Jefferies, 2013; Hoffman et al., 2018), in left-hemisphere semantic areas such as inferior frontal gyrus and posterior temporal gyrus, as well as in medial temporal lobes, medial prefrontal and posterior cingulate cortex (Figure 2A).

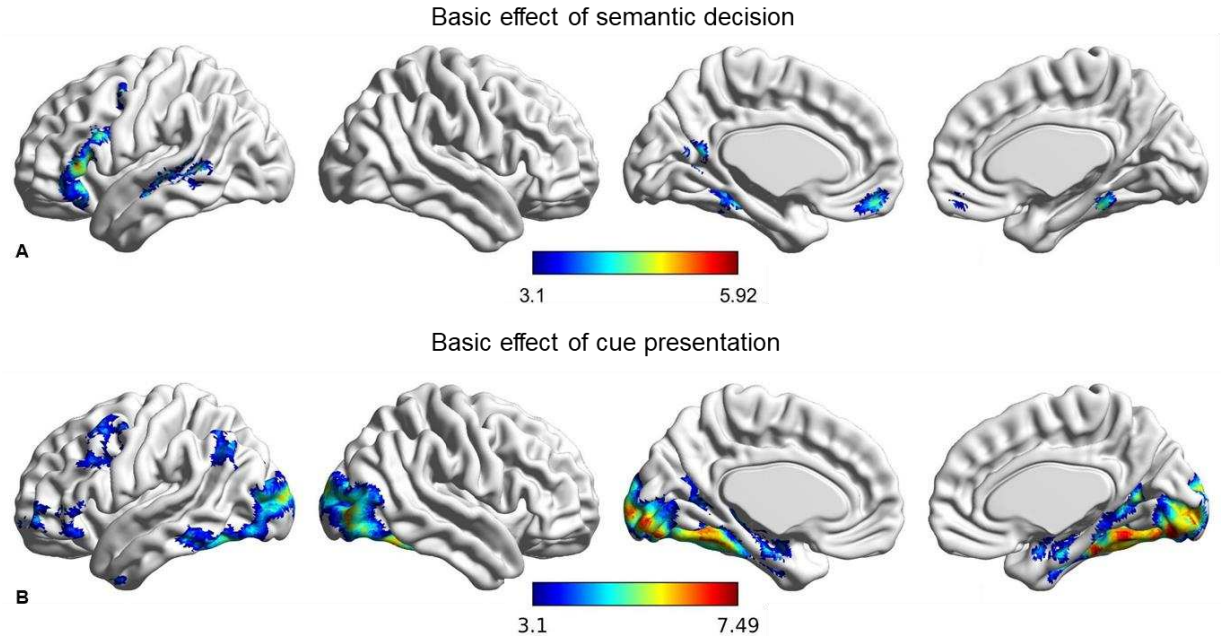

Figure 2. A. Basic effect of uncued semantic decision (semantic no cue > letter strings at decision time period). B. Basic effect of cue presentation (2 cues + 1 cue > 0 cue at cue time period). Coordinates of cluster peaks for these basic comparisons are reported in Table S3.

We then explored cueing effects by contrasting semantic decisions in the presence of different levels of constraint. The contrast of semantic decisions following 1 cue > 0 cues identified clusters in task-positive regions overlapping with the MDN (Duncan, 2010), consistent with the cognitive demands of maintaining cues. We found recruitment of inferior and middle frontal gyrus (with the peak in inferior frontal sulcus), precentral gyrus, bilateral paracingulate gyrus and pre-supplementary motor area, temporo-occipital cortex and visual cortex. Interestingly, the effect of multiple cues compared with a single cue (2>1) did not elicit stronger activation within these regions, even though the amount of information to be maintained was increased. Instead, this contrast elicited activation in regions overlapping with the DMN, including in bilateral angular gyrus/lateral occipital cortex, middle temporal gyrus, medial prefrontal cortex, posterior cingulate cortex, and left middle frontal gyrus. The thresholded maps for the two contrasts can be found in Figure 3 (top panel). Parameter estimates for the three conditions over the implicit baseline were extracted in both the 1>0 cue and 2>1 cue regions (see Supplementary Figure S4). Overall, 1>0 regions showed task-related activation (with more activation when cues had to be maintained in working memory, compared with the no cue condition) while 2>1 regions exhibited task-related deactivation (with less deactivation when people made semantic decisions following 2 convergent cues compared with 0 or 1 cue).

We examined the overlap of the contrast maps with published maps of the MDN (Duncan, 2010) and DMN (Yeo et al., 2011; Figure 3 - bottom). Consistent with the hypothesized role of DMN in semantic integration, 36.2% of the total voxels in the 2>1 cue map overlapped with the DMN, while only 1% of voxels overlapped with MDN. For the 1>0 cue map, the opposite pattern was observed, with 31.8% of total voxels overlapping with MDN and only 2.4 % with DMN. We submitted the unthresholded z maps for the 2>1 and 1>0 cue contrasts to Neurosynth for cognitive decoding and produced word clouds using the top 10 terms positively associated with the maps (Figure 3 – middle). The terms recovered for the 2>1 and 1>0 cue maps suggest the involvement of DMN and MDN respectively. The contrast of 2 > 0 cues (Figure S3), shows activation in regions overlapping with 1 > 0, such as left middle and inferior frontal gyrus, left middle temporal gyrus, but also in regions within the 2 > 1 map, such as left angular gyrus. This pattern of activation suggests that both cue mainteinance and cue integration might be visible in this map.

As the DMN is known to show anti-correlation with task-positive regions captured by the MDN (Blank et al., 2014; Davey et al., 2016; Fox et al., 2005), we also explored whether this would be the case for our contrast maps. In an independent sample of 86 participants, whole-brain connectivity maps for the 2>1 and 1>0 contrasts were generated using CONN (Whitfield-Gabrieli & Nieto-Castanon, 2012). Full methods are in the Supplementary Materials. The analysis revealed two functionally distinct and anti-correlated networks, comprising DMN for the 2>1 cue contrast and MDN regions involved in domain-general executive control for the 1>0 cue contrast (Figure S5).

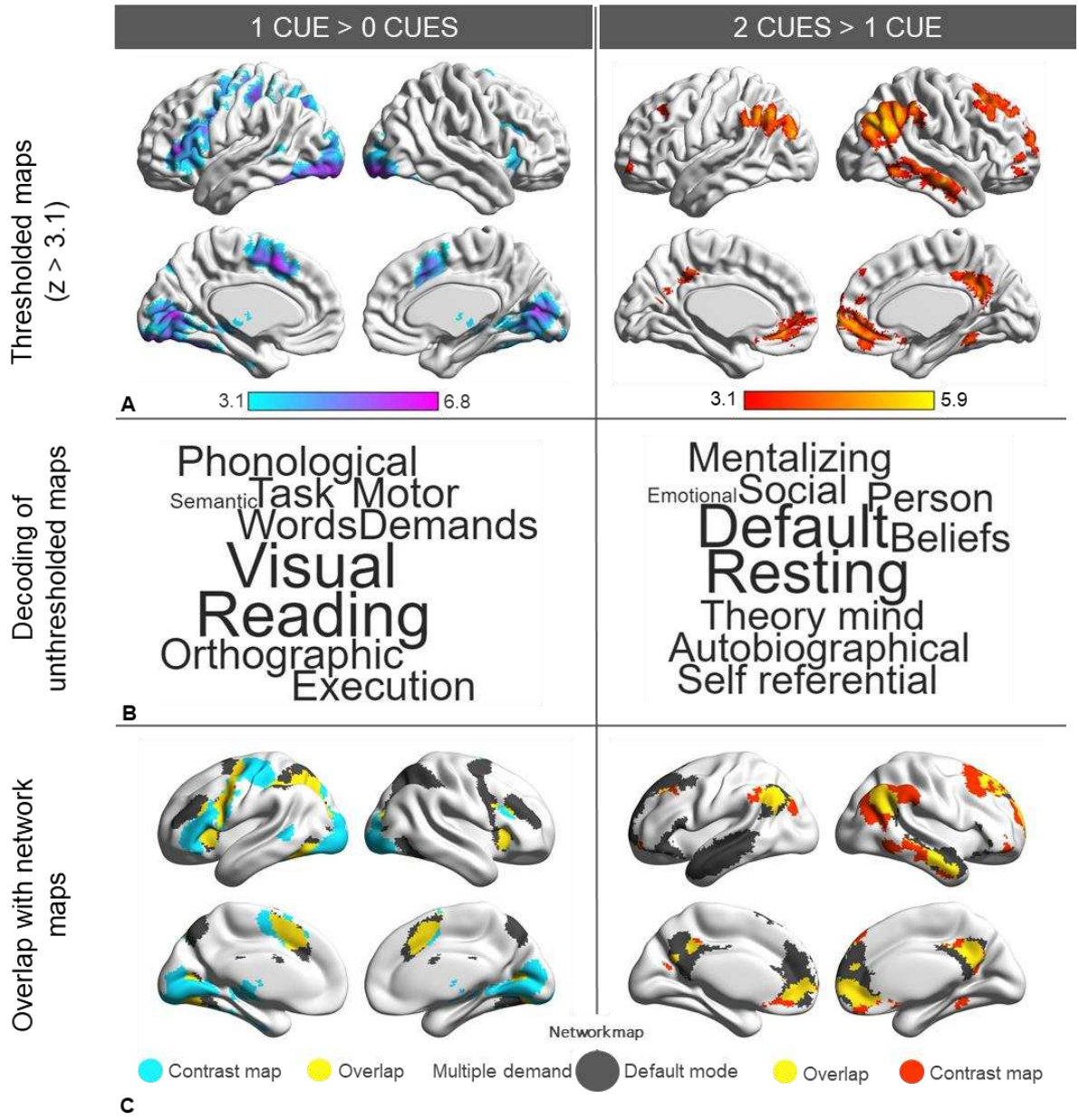

Figure 3. Results for the main contrasts of interest in the semantic decision model: the left side of the figure contains results for 1 cue > 0 cues, while the 2 cues > 1 cue contrast is shown on the right. A. Contrast maps thresholded at z > 3.1. B. Word clouds produced by plotting the top 10 terms positively associated with the contrast map. C. Overlap of the 1 > 0 contrast with the multiple demand network (Duncan et al., 2010) and the contrast of 2 >1 with the default mode network (Yeo et al., 2011).

Cue model

To check whether the two distinct networks identified as relevant for conceptual cueing also showed different responses to load during the encoding of cue information, we constructed a second model to look at the cue presentation period. This was an exploratory analysis, since our main focus was on how cues modulate the neural basis of semantic decisions. Our

paradigm was not designed to deconfound the order of the cues and the semantic decisions. Nevertheless, if the regions showing a stronger response to semantic decisions following 1 vs. 0 cues reflect the working memory demands of cue maintenance, we would expect to see load-dependent effects from cue encoding in these regions – i.e. stronger responses when more cues are presented.

First, we used a contrast of 2 cues + 1 cue > 0 cues across the whole brain to define the basic effect of cue presentation (see Figure 2B). This elicited bilateral activation in occipital visual regions, extending into the posterior ventral stream in the left hemisphere. In addition, we found bilateral recruitment of the inferior frontal sulcus (IFS), within the multiple demand network, and the inferior frontal gyrus, in line with the idea of load demands of processing and maintaining cues (this interpretation is further explored in paragraph 3.2.2 'ROI analysis of cue load). Activation in the left hemisphere was also observed in AG.

The Supplementary Figure S2 shows other cue presentation contrasts. The contrast of 2 > 0 cue presentation revealed activation in occipital cortex and in left-hemisphere control regions. Similar control regions were recruited by the contrast of 2 > 1 cue presentation, although this map had less extensive activation overall. The contrast of 1 cue > 0 cue presentation revealed activity in visual regions largely overlapping with 2 cues > 0 cues, and a cluster in left angular gyrus. Finally, the contrast of 1 cue location > 1 cue affect recruited visual regions in occipital cortex and bilateral paracingulate gyrus, while the reverse contrast did not yield significant results.

3.2.2 ROI analysis of cue load

To test possible accounts of the different patterns of activation observed in the decision-making phase (*semantic decision model*) for the contrasts of 2 > 1 and 1 > 0 cues, we conducted a post-hoc ROI analysis of the activation in these regions prior to the decision, when the cues were on the screen (*cue model*). The recruitment of cognitive control areas (i.e. inferior and middle frontal gyrus, inferior frontal sulcus, precentral gyrus, anterior cingulate gyrus, and pre-supplementary motor area, falling within the multiple demand network) for semantic decisions that followed the presence vs. absence of cues (1 > 0 cues) suggests that these regions might be engaged in active maintenance of task-relevant information; in which case, cues might be processed in a load-dependent way during the cue period. To test this idea, the regions that

responded to the contrasts of 1>0 and 2>1 cues during the semantic task (semantic decision model) were used to mask the BOLD response for cue presentation (cue model). We extracted and compared the parameter estimates for the three conditions against the implicit baseline: no cues (scrambled images), one cue (average of face emotion and location cue) and two cues (both face emotion and location image presented). If the semantic task activation observed for the 1>0 contrast reflects a demand-relevant state associated with maintaining the cues, then the activation of these regions during cue presentation should increase as the number of cues is increased; i.e. 2 cues > 1 cue, 1 cue > 0 cues. This is because information about the cues is required to be maintained from their onset. In contrast, regions responding more to semantic decisions following multiple cues (2>1 cues) might not be expected to show a load-dependent effect during the cue period. These regions responded more when multiple sources of information could be used to constrain semantic retrieval – and this form of information integration is unlikely to occur prior to the onset of the semantic decision (since the cues themselves were not easy to link in the absence of the probe concept – for example HAPPY FACE and SUPERMARKET are consistent with a wide range of concepts and do not strongly prime JAM). Consistent with these predictions, we found that activation in the 1>0 cue regions increased in a linear fashion with a higher number of cues [$F (1, 25) = 48.39$, $p < .001$, $\eta^2 = .66$] (Figure 4A). However, there was no significant difference between cue conditions within regions responsive to the 2>1 cue contrast [$F (2, 50) = .39$, $p = .682$, $\eta^2 = .02$] (Figure 4D).

The results of this ROI analysis show that regions responding more to semantic decisions following 1 > 0 cues also respond in a load-dependent way during the encoding of cue information. However, this ROI map includes both cognitive control regions within MDN and visual cortex, making it difficult to separate the effects of increasing visual stimulation from cognitive load. To further characterize the effect, we divided the 1 > 0 semantic decision map into regions that fell within the occipital cortex (Harvard-Oxford probabilistic map – 25%) and outside MDN regions (1997 voxels – Figure 4B), and within MDN after masking out occipital regions (10658 voxels – Figure 4C). The BOLD response showed a similar linear increase with the number of cues presented on the screen in visual cortex ($F (1, 25) = 54.96$, $p < .001$, $\eta^2 = .69$) and in MDN ($F (1, 25) = 53.73$, $p < .001$, $\eta^2 = .68$).

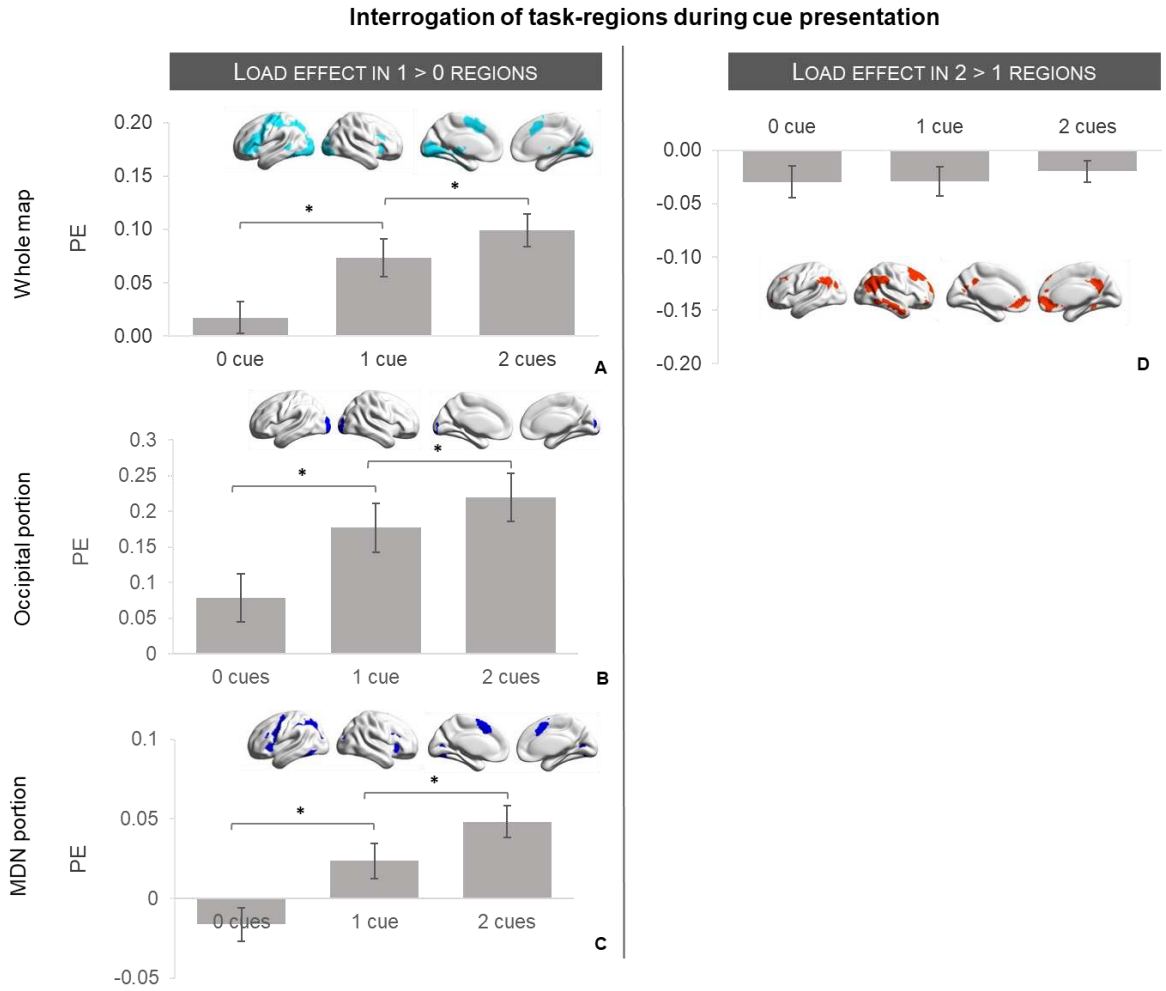

Fig 4. ROI analysis extracting the parameter estimates (PE) for the three levels of cue processing over the implicit baseline (cue model) in the 1 > 0 and 2 > 1 maps obtained in the semantic decision model. Three separate ROIs were conducted for the 1 > 0 regions (left panel): whole map (A), voxels that fell within the occipital cortex (B) and voxels that fell in the MDN (C). While the effect of number of cues is present in the 1 > 0 regions across the different masks used, no effect is observed in the integration regions (D) at the time-point of processing cue pictures. Bonferroni-corrected pairwise comparisons in the 1 > 0 regions confirmed that PE for 0 cues were significantly lower than 1 cue, and PE for 1 cue were significantly lower than 2 cues (all p values < .025; p value corrected for 2 multiple comparisons).

3.2.3 Gradient analysis

To further characterize the involvement of DMN regions in integrating information, we interrogated the response to semantic decisions along the Principal Gradient (Margulies et al., 2016). Unlike traditional univariate activation maps, which localize activation in certain regions, this gradient analysis examines how the effect of cueing unfolds along the entire cortical surface and measures the contribution of different portions of the gradient to the effects of

interest. This analysis can highlight systematic functional change along the cortical surface, and explain why similar functional transitions are observed in multiple locations. The gradient map was divided into 10-percentile bins (see Methods section) and each bin was used as a mask in ROI analyses where we extracted mean parameter estimates for the contrasts of 2 cues vs. 1 cue and 1 cue vs. 0 cues within each bin (see Figure 5). We then explored the effect of gradient bin on each univariate contrast using a two-way repeated measure ANOVA with *cue contrast* (2 levels: 2 cues vs.1 cue and 1 cue vs. 0 cues) and *gradient bin* (10 levels) as within-subject variables. This analysis revealed a significant interaction of cue contrast and gradient bin ($F(2, 51) = 28.33$, $p < .001$, $\eta^2 = .53$), suggesting that the effect of gradient was different for 2 > 1 and 1 > 0 contrasts. Next, we performed two one-way repeated measure ANOVAs looking at the effect of *gradient bin* on each contrast separately. For 2>1 cues, we found a significant linear effect for gradient bin ($F(1, 25) = 47.13$, $p < .001$, $\eta^2 = .65$), as well as complex higher-order contrast effects (values reported in Table S5). The comparison of semantic decisions following 2 vs. 1 cues elicited maximal activity at the heteromodal end of the gradient, suggesting that DMN regions at this end of the principal gradient responded more strongly when multiple sources of information were integrated to support semantic cognition. For 1>0 cues, we found the opposite pattern, with more activation at the unimodal end of the gradient for the single cue condition compared to when no cues were provided. Again, the effect of context vs. no-context along the principal gradient was complex, with linear ($F(1, 25) = 24.80$, $p < .001$, $\eta^2 = .50$), as well as higher-order contrasts reaching significance. Full details of the statistical outcomes are reported in Supplementary Tables S4, S5, S6.

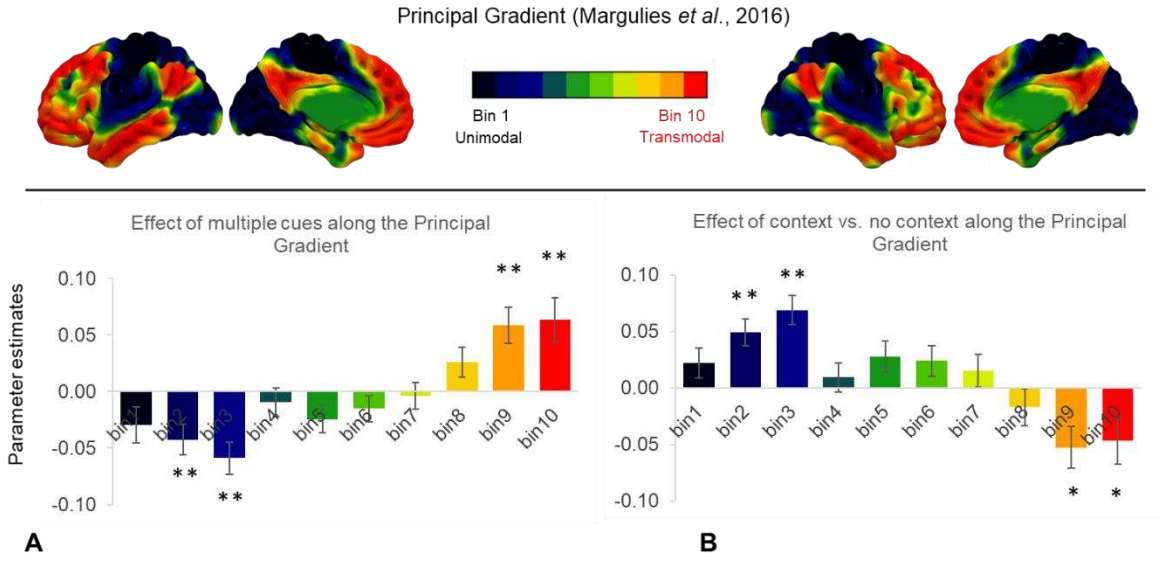

Figure 5. A. Semantic decisions in the presence of multiple cues (contrast of 2>1 cues) maximally recruited regions at the heteromodal end of the principal gradient. B. The effect of context vs. no context (contrast of 1>0 cues) showed an effect in the opposite direction, with maximal activation toward the sensory end of the gradient. ** Highlights portions of the gradient where the BOLD response is significantly different from 0 when the Bonferroni correction is applied (all p values ≤ .005), while * denotes p values < .05.

4 DISCUSSION

Recent accounts of the default mode network (DMN) place this system at the top of a cortical hierarchy, maximally distant from unimodal sensory regions (Margulies et al., 2016) in both geodesic and connectivity space. The separation of heteromodal DMN regions from unimodal cortex may underpin our capacity to form conceptual representations that are not dominated by a particular type of feature but instead draw on multiple types of information – including affect or spatial location. To test this idea, we contrasted semantic decisions made following the presentation of multiple cues (depicting facial emotional expressions and locations), only one of these cues, or no cues. In this way, we manipulated the extent to which semantic retrieval occurred in a rich and meaningful context, in which multiple convergent features were available. Our results indicate that the cueing paradigm involved distinct mental processes that were supported by different networks. First, from the onset of the cues, information was maintained in working memory: MDN regions were activated for the contrast 1 cue > 0 cues, and the response of these regions during cue presentation was load-dependent. These findings are in line with previous research showing that the multiple demand network supports the maintenance of goal-relevant information (Duncan, 2010; Woolgar et al., 2011). Secondly, DMN regions were activated by the contrast 2 cues > 1 cue, consistent with a role of this network in convergent information integration. In line with our prediction that information integration occurs at the heteromodal end of the Principal Gradient, we found greater recruitment at this end when semantic decisions occurred in the presence of multiple cues. In contrast, activation was greater towards the unimodal end of the gradient (in regions overlapping with visual cortex) when semantic decisions were made in the presence vs. absence of cues. These novel findings provide important insights into the neural mechanisms supporting semantic integration and suggest a framework for understanding the location of these effects at the heteromodal end of the principal gradient.

According to "task-negative" accounts of the DMN, apparent semantic activation of this network occurs when an easy task is contrasted with a hard task (Humphreys et al., 2015; Humphreys et al., 2019; Humphreys & Lambon Ralph, 2014). This account is unlikely to provide an adequate explanation of our data since we found no behavioural differences between conditions (unlike other reports of cueing effects; Lanzoni et al., 2019; Noonan et al., 2010; Rodd et al., 2016, 2013). Our findings are instead consistent with a rich neuroimaging literature implicating ATL and AG in the formation of conceptual combinations. Integrating items (e.g. "jacket" and "plaid") into coherent concepts (i.e. "plaid jacket") modulates activity in AG regardless of the modality of presentation, while atrophy in this region results in impaired conceptual combinations (Price et al., 2015; see also Price et al., 2016). Similarly, magnetoencephalography (MEG) studies show increased activity in left ATL and AG for meaningful conceptual combinations (e.g. "red boat") compared to the same words preceded by unpronounceable consonant strings (e.g. "xkq boat; Bemis & Pylkkänen, 2011; 2013; Pylkkänen, 2019), particularly when these combinations are more predictable or share more overlapping semantic features (Teige et al., 2019). Activation in the left superior ATL is also observed during semantic decisions following meaningful sentence cues, while IFG shows the opposite pattern (i.e. increased activation following irrelevant vs. relevant contexts), consistent with a role in semantic control (Hoffman et al., 2015). Moving beyond the language stimuli used in previous studies on conceptual combinations, here we show that semantic integration in DMN occurs for non-verbal material (i.e. pictures), in line with the heteromodal nature of these regions. Our findings uniquely add to this literature by showing that these effects of conceptual combination are maximal at the heteromodal end of the principal gradient, which situates DMN at the top of functional hierarchy (Margulies et al., 2016). Consequently, effects of information integration are seen not only in classic semantic regions such as AG and anterior middle temporal gyrus, but also in other DMN regions highlighted by our 2 > 1 cues contrast (e.g., superior frontal gyrus; medial prefrontal and posterior cingulate cortex).

The role of DMN in semantic cognition appeared to be largely restricted to the impact of convergent cueing during semantic decision-making: in contrast, a distinct anti-correlated network overlapping with MDN was associated with the selective attention and working memory demands of encoding and maintaining individual cues. Moreover, the basic effect of making semantic decisions in the absence of cues, relative to the letter string trials, did not

reveal activation in DMN regions. At first, this result may seem at odds with accounts of the DMN that attribute a crucial role in semantic cognition to this network. However, our semantic task was considerably more demanding than the letter string baseline: studies have shown that although DMN regions can respond to the contrast of semantic vs. non-semantic tasks, they typically do so when the semantic task is not more demanding than the comparison task (Binder et al., 2009; Humphreys et al., 2015). Moreover, activation in DMN regions is often associated with 'automatic' patterns of retrieval or conceptual combinations (Davey et al., 2016; Teige et al., 2019; Price et al., 2016, Bemis & Pylkkänen, 2011; 2013), while our task required participants to match an ambiguous words to a target word while discarding distractors and as such, it might involve more 'controlled' aspects of retrieval supported by regions such as left IFG which lie outside DMN.

In line with other studies, we found that DMN regions responding to cue integration (i.e. the 2>1 cue contrast during semantic decisions) showed differential deactivation across conditions, relative to the implicit baseline, while MDN regions responding to cue maintenance (i.e., the 1>0 cue contrast during semantic decisions) showed differential activation. The functional significance of task-related deactivation is a topic of considerable debate; while some authors have interpreted deactivation as suggesting that sites are irrelevant to ongoing cognition (e.g. Humphreys et al., 2015), another possibility is that deactivation might be functionally relevant, as it might allow DMN regions to integrate information more selectively from task-relevant networks (Krieger-Redwood et al., 2016). According to this "cognitive tuning" hypothesis, we might expect more deactivation of DMN regions when only a limited set of features are relevant to ongoing cognition (for example, in the 0 and 1 cue conditions, when emotion and location representations are not necessarily task-relevant). There are already studies demonstrating that DMN regions can increase their coupling to cognitive control areas when harder tasks are contrasted with easier tasks, even as they deactivate (Krieger-Redwood et al., 2016; Vatansever et al., 2015; 2017).

The effect of convergent cueing was not found within one specific semantic region, such as AG, but across multiple distributed nodes of DMN. We then turned to the Principal Gradient of intrinsic connectivity to provide a potential explanation for why cue integration effects were observed where they were across the cortex. The separation between DMN and unimodal systems, captured by the Principal Gradient, is thought to (i) allow heteromodal

representations to emerge (cf. Hub and Spoke account) and (ii) support forms of cognition that require separation from the external environment, such as states that draw on heteromodal representations in memory. The latter observation is particularly important for explaining the similarity of our results with recent findings from our group (Murphy et al., 2018, 2019). Using a 1-back/0-back paradigm, Murphy et al. showed that decisions based on the immediately available perceptual input (0 back condition) elicited higher activity towards the unimodal end of the Principal Gradient, while decisions drawing on information from memory (1 back condition) maximally recruited the heteromodal end of the gradient (Murphy et al., 2019). Critically, DMN involvement in memory-guided cognition was maximised when the decisions involved meaningful objects that were not perceptually-identical, increasing reliance on conceptual knowledge, relative to simpler unidimensional decisions based on colour (Murphy et al., 2018). Building on these findings, the results of the current study suggest that this pattern of activation within DMN arises because heteromodal cortex at the top end of the gradient supports the integration of disparate and convergent sources of information; these regions are more involved when we match meaningful objects based on their identities extracted from a multitude of features, as opposed to single features. Nevertheless, Murphy et al. also showed that tasks based on memory recruit representations at the heteromodal end of the gradient, even when these tasks only probe a single feature and therefore arguably do not place strong demands on information integration: this pattern might arise because in the absence of perceptual inputs, heteromodal regions may play a key role in generating patterns of cognition needed for the task (i.e., visual imagery). Importantly, the regions at the top of the gradient responded similarly to memory-based decisions irrespective of whether these decisions concerned colour or shape; in this way, the function of these sites still reflects the heteromodal nature of DMN. In contrast, distinct unimodal sites responsive to colour and shape are expected to support these decisions when perceptual information is present. In summary, the principal gradient relating to the separation of heteromodal from unimodal processing can potentially explain both the increased response in heteromodal DMN when cognition involves multiple convergent features, and the common response in heteromodal DMN when cognition involves decisions about single features in the absence of perceptual input.

There are a number of limitations of this study. It does not fully establish the form of the relationship between the number of cues and DMN activation at retrieval, since we did not manipulate cueing parametrically. Activation in DMN regions may not increase linearly with the number of cues (0, 1, 2 cues). Instead, the contrast of 1 > 0 cues elicits activation in MDN regions and towards the unimodal end of the principal gradient, suggesting that the presence vs. absence of context involves additional cue encoding and maintenance in working memory. A follow up study could use a parametric manipulation of the number of cues to better identify how responses in MDN and DMN scale with the number of cues. Moreover, in our experiment, integration unfolded over time, with semantic decisions occurring roughly 2 seconds after the presentation of the cue. A recent study by Branzi and others (2019) suggests that ventral AG supports the integration of meanings during time-extended narratives (see also Bonnici et al., 2016; Ramanan et al., 2017). Future research should establish whether semantic integration that emerges over time leads to a different pattern of activation along the principal gradient compared with the integration of simultaneously-presented information.

Furthermore, although our cueing paradigm allowed us to recover a set of regions within DMN recruited during semantic integration, it is unclear whether we would observe the same pattern of activation with other types of cues. Future studies could examine tasks that involve simple sensory features, for example, semantic decisions about concrete concepts such as DOG following visual and auditory feature cues (e.g. image of tail and sound of dog barking) to establish if a similar integration effect occurs in DMN. The current experiment used complex stimuli depicting emotional affect and locations, which are known to be relevant to the DMN. The DMN is closely associated with the classic limbic network for emotional processing (e.g. Chanes & Barrett, 2016; Greicius et al., 2003; Raichle et al., 2001; Simpson et al., 2000). Moreover, the hippocampus, which has strong functional ties with the default mode network (Andrews-Hanna et al., 2010; Kernbach et al., 2018 ; Leech & Sharp, 2014; Raichle et al., 2001) is known to play a role in representing spatial locations (e.g. Bellmund et al., 2016; Burgess, 2002; Burgess et al., 2002; Robin et al., 2018). Our findings demonstrate that when semantic decisions are made in the context of both emotional and spatial information, as opposed to only one of these cue types, DMN ramps up its response in line with its hypothesised role in higher-order information integration. Contrary to previous literature showing the recruitment of the parahippocampal place area for spatial scenes (e.g. Epstein & Kanwisher, 1998) and the

fusiform face area for faces (e.g. Kanwisher et al., 1997), our contrasts of 1 cue type over the other aligned only partially with previous evidence. The failure to reach statistical significance for the contrast of 1 cue affect > 1 cue location could reflect a lack of statistical power, since much of the data acquisition was devoted to the semantic decisions. Moreover, the different size and aspect ratio of the images (with location images being wider and larger) may have influenced the results.

A final limitation of the study concerns the statistical model used to examine activation during cue presentation, which was used to test possible interpretations of the univariate results in the main model in a post-hoc fashion. As the experiment was not originally designed to look at the cue presentation, we did not include trials in which facial expressions and location cues were not followed by semantic decisions. Whenever a meaningful cue picture was presented, this was always followed by a semantic decision. The inclusion of trials where cues were followed by a blank screen would have facilitated the temporal separation of the cue and task events, allowing us to draw stronger conclusions from the cue model. In this way, future research could directly test the idea that integration requires a component of maintenance supported by the MDN, in addition to a combination of conceptual features within DMN.

BIBLIOGRAPHY

Andrews-Hanna, J. R., Reidler, J. S., Sepulcre, J., Poulin, R., & Buckner, R. L. (2010). Functional-Anatomic Fractionation of the Brain's Default Network. *Neuron*, *65*(4), 550–562. https://doi.org/10.1016/j.neuron.2010.02.005

Badre, D., & Wagner, A. D. (2005). Frontal lobe mechanisms that resolve proactive interference. *Cerebral Cortex*, *15*(12), 2003–2012. https://doi.org/10.1093/cercor/bhi075

Badre, D., & Wagner, A. D. (2006). Computational and neurobiological mechanisms underlying cognitive flexibility. *Proceedings of the National Academy of Sciences of the United States of America*, *103*(18), 7186–7191. https://doi.org/10.1073/pnas.0509550103

Beckmann, C. F., Jenkinson, M., & Smith, S. M. (2003). General multilevel linear modeling for group analysis in FMRI. *NeuroImage*, *20*(2), 1052–1063. https://doi.org/10.1016/S1053-8119(03)00435-X

Behzadi, Y., Restom, K., Liau, J., & Liu, T. T. (2007). A component based noise correction method (CompCor) for BOLD and perfusion based fMRI. *NeuroImage*, *37*(1), 90–101. https://doi.org/10.1016/j.neuroimage.2007.04.042

Bellmund, J. L. S., Deuker, L., Schröder, T. N., & Doeller, C. F. (2016). Grid-cell representations in mental simulation. *ELife*, *5*(AUGUST), 1–21. https://doi.org/10.7554/eLife.17089

Bemis, D. K., & Pylkkänen, L. (2011). Simple Composition: A Magnetoencephalography Investigation into the Comprehension of Minimal Linguistic Phrases. *Journal of Neuroscience*, *31*(8), 2801–2814. https://doi.org/10.1523/JNEUROSCI.5003-10.2011

Bemis, D. K., & Pylkkänen, L. (2013). Basic linguistic composition recruits the left anterior temporal lobe and left angular gyrus during both listening and reading. *Cerebral Cortex*, *23*(8), 1859–1873. https://doi.org/10.1093/cercor/bhs170

Binder, J. R., Desai, R. H., Graves, W. W., & Conant, L. L. (2009). Where Is the Semantic System? A Critical Review and Meta-Analysis of 120 Functional Neuroimaging Studies. *Cerebral Cortex*, *19*(12), 2767–2796. https://doi.org/10.1093/cercor/bhp055

699 Blank, I., Kanwisher, N., & Fedorenko, E. (2014). A functional dissociation between language
700 and multiple-demand systems revealed in patterns of BOLD signal fluctuations. *Journal*
701 *of Neurophysiology*, *112*(5), 1105–1118. https://doi.org/10.1152/jn.00884.2013

702 Bonnici, H. M., Richter, F. R., Yazar, Y., & Simons, J. S. (2016). Multimodal Feature Integration
703 in the Angular Gyrus during Episodic and Semantic Retrieval. *Journal of Neuroscience*,
704 *36*(20), 5462–5471. https://doi.org/10.1523/JNEUROSCI.4310-15.2016

705 Branzi, F. M., Humphreys, G. F., Hoffman, P., & Ralph, M. A. L. (2019). Revealing the neural
706 networks that extract conceptual gestalts from continuously evolving or changing
707 semantic contexts. *BioRxiv*, 666370. https://doi.org/10.1101/666370

708 Bright, P., Moss, H., & Tyler, L. K. (2004). Unitary vs multiple semantics: PET studies of word
709 and picture processing. *Brain and language*, *89*(3), 417-432.
710 https://doi.org/10.1016/j.bandl.2004.01.010

711 Brysbaert, M., Warriner, A. B., & Kuperman, V. (2014). Concreteness ratings for 40 thousand
712 generally known English word lemmas. Behavior research methods, 46(3), 904-911.
713 https://doi.org/10.3758/s13428-013-0403-5

714 Buckner, R. L., & Krienen, F. M. (2013). The evolution of distributed association networks in
715 the human brain. *Trends in Cognitive Sciences*, *17*(12), 648–665.
716 https://doi.org/10.1016/j.tics.2013.09.017

717 Burgess, N. (2002). The hippocampus, space, and viewpoints in episodic memory. *The*
718 *Quarterly Journal of Experimental Psychology Section A*, *55*(4), 1057–1080.
719 https://doi.org/10.1080/02724980244000224

720 Burgess, N., Maguire, E. A., & O'keefe, J. (2002). Review The Human Hippocampus and Spatial
721 and Episodic Memory appears to remain in humans (Abrahams et al. *Neuron*, *35*, 625–
722 641. https://doi.org/10.1016/S0896-6273(02)00830-9

723 Chai, X. J., Castañán, A. N., Öngür, D., & Whitfield-Gabrieli, S. (2012). Anticorrelations in
724 resting state networks without global signal regression. *NeuroImage*, *59*(2), 1420–1428.
725 https://doi.org/10.1016/j.neuroimage.2011.08.048

726 Chanes, L., & Barrett, L. F. (2016). Redefining the Role of Limbic Areas in Cortical Processing.

Trends in Cognitive Sciences, *20*(2), 96–106. https://doi.org/10.1016/j.tics.2015.11.005

Chee, M. W., Weekes, B., Lee, K. M., Soon, C. S., Schreiber, A., Hoon, J. J., & Chee, M. (2000). Overlap and dissociation of semantic processing of Chinese characters, English words, and pictures: evidence from fMRI. *Neuroimage*, *12*(4), 392-403. https://doi.org/10.1006/nimg.2000.0631

Chiou, R., & Lambon Ralph, M. A. (2019). Unveiling the dynamic interplay between the hub- and spoke-components of the brain's semantic system and its impact on human behaviour. *NeuroImage*, *199*(April), 114–126. https://doi.org/10.1016/j.neuroimage.2019.05.059

Davey, J., Cornelissen, P. L., Thompson, H. E., Sonkusare, S., Hallam, G., Smallwood, J., & Jefferies, E. (2015). Automatic and Controlled Semantic Retrieval: TMS Reveals Distinct Contributions of Posterior Middle Temporal Gyrus and Angular Gyrus. *The Journal of Neuroscience : The Official Journal of the Society for Neuroscience*, *35*(46), 15230–15239. https://doi.org/10.1523/JNEUROSCI.4705-14.2015

Davey, J., Thompson, H. E., Hallam, G., Karapanagiotidis, T., Murphy, C., De Caso, I., … Jefferies, E. (2016). Exploring the role of the posterior middle temporal gyrus in semantic cognition: Integration of anterior temporal lobe with executive processes. *NeuroImage*, *137*, 165–177. https://doi.org/10.1016/j.neuroimage.2016.05.051

Dosenbach, N. U., Visscher, K. M., Palmer, E. D., Miezin, F. M., Wenger, K. K., Kang, H. C., ... & Petersen, S. E. (2006). A core system for the implementation of task sets. Neuron, 50(5), 799-812. https://doi.org/10.1016/j.neuron.2006.04.031

Dumontheil, I., Thompson, R., & Duncan, J. (2011). Assembly and use of new task rules in fronto-parietal cortex. *Journal of Cognitive Neuroscience*, *23*(1), 168-182. https://doi.org/10.1162/jocn.2010.21439

Duncan, J. (2010). The multiple-demand (MD) system of the primate brain: mental programs for intelligent behaviour. *Trends in Cognitive Sciences*, *14*(4), 172–179. https://doi.org/10.1016/j.tics.2010.01.004

Epstein, R., & Kanwisher, N. (1998). A cortical representation of the local visual environment. Nature, 392(6676), 598-601. https://doi.org/10.1038/33402

Fox, M. D., Snyder, A. Z., Vincent, J. L., Corbetta, M., Van Essen, D. C., & Raichle, M. E. (2005). The human brain is intrinsically organized into dynamic, anticorrelated functional networks. *Proceedings of the National Academy of Sciences of the United States of America*, *102*(27), 9673–9678. https://doi.org/10.1073/pnas.0504136102

Gawlick-Grendell, L. A., & Woltz, D. J. (1994). Meaning dominance norms for 120 homographs. *Behavior Research Methods, Instruments, & Computers*, *26*(1), 5–25. https://doi.org/10.3758/BF03204557

Gold, B. T., Balota, D. A., Kirchhoff, B. A., & Buckner, R. L. (2005). Common and dissociable activation patterns associated with controlled semantic and phonological processing: evidence from FMRI adaptation. *Cerebral Cortex*, *15*(9), 1438-1450. https://doi.org/10.1093/cercor/bhi024

Greicius, M. D., Krasnow, B., Reiss, A. L., & Menon, V. (2003). Functional connectivity in the resting brain: A network analysis of the default mode hypothesis. *Proceedings of the National Academy of Sciences of the United States of America*, *100*(1), 253–258. https://doi.org/10.1073/pnas.0135058100

Hallam, G. P., Whitney, C., Hymers, M., Gouws, A. D., & Jefferies, E. (2016). Charting the effects of TMS with fMRI: Modulation of cortical recruitment within the distributed network supporting semantic control. *Neuropsychologia*, *93*(September), 40–52. https://doi.org/10.1016/j.neuropsychologia.2016.09.012

Hoffman, P., Binney, R. J., & Ralph, M. A. L. (2015). Differing contributions of inferior prefrontal and anterior temporal cortex to concrete and abstract conceptual knowledge. *Cortex*, *63*, 250-266. https://doi.org/10.1016/j.cortex.2014.09.001

Hoffman, P., McClelland, J. L., & Lambon Ralph, M. A. (2018). Concepts, control, and context: A connectionist account of normal and disordered semantic cognition. *Psychological Review*, *125*(3), 293–328. https://doi.org/10.1037/rev0000094

Humphreys, G. F., Hoffman, P., Visser, M., Binney, R. J., & Lambon Ralph, M. A. (2015). Establishing task- and modality-dependent dissociations between the semantic and default mode networks. *Proceedings of the National Academy of Sciences*, *112*(25), 7857–7862. https://doi.org/10.1073/pnas.1422760112

785 Humphreys, G. F., Jackson, R. L., & Ralph, M. A. L. (2019). Overarching principles and
786 dimensions of the functional organisation in the inferior parietal cortex. *BioRxiv*, *44*(0).
787 https://doi.org/10.1101/654178

788 Humphreys, G. F., & Lambon Ralph, M. A. (2014). Fusion and fission of cognitive functions in
789 the human parietal cortex. *Cerebral Cortex*, *25*(10), 3547–3560.
790 https://doi.org/10.1093/cercor/bhu198

791 Jackson, R. L., Hoffman, P., Pobric, G., & Lambon Ralph, M. A. (2016). The Semantic Network
792 at Work and Rest: Differential Connectivity of Anterior Temporal Lobe Subregions. *The*
793 *Journal of Neuroscience : The Official Journal of the Society for Neuroscience*, *36*(5),
794 1490–1501. https://doi.org/10.1523/JNEUROSCI.2999-15.2016

795 Jefferies, E. (2013). The neural basis of semantic cognition: Converging evidence from
796 neuropsychology, neuroimaging and TMS. *Cortex*, *49*(3), 611–625.
797 https://doi.org/10.1016/j.cortex.2012.10.008

798 Jenkinson, M., Bannister, P., Brady, M., & Smith, S. (2002). Improved Optimization for the
799 Robust and Accurate Linear Registration and Motion Correction of Brain Images.
800 *NeuroImage*, *17*(2), 825–841. https://doi.org/10.1006/nimg.2002.1132

801 Jenkinson, M., & Smith, S. (2001). A global optimisation method for robust affine registration
802 of brain images. *Medical Image Analysis*, *5*(2), 143–156. https://doi.org/10.1016/S1361-
803 8415(01)00036-6

804 Kanwisher, N., McDermott, J., & Chun, M. M. (1997). The fusiform face area: a module in
805 human extrastriate cortex specialized for face perception. Journal of neuroscience,
806 17(11), 4302-4311. https://doi.org/10.1523/JNEUROSCI.17-11-04302.1997

807 Kernbach, J. M., Gramfort, A., Thirion, B., Thiebaut de Schotten, M., Sabuncu, M. R., Yeo, B. T.
808 T., … Margulies, D. S. (2018). Subspecialization within default mode nodes characterized
809 in 10,000 UK Biobank participants. *Proceedings of the National Academy of Sciences*,
810 *115*(48), 12295–12300. https://doi.org/10.1073/pnas.1804876115

811 Krieger-Redwood, K., Teige, C., Davey, J., Hymers, M., & Jefferies, E. (2015). Conceptual
812 control across modalities: Graded specialisation for pictures and words in inferior frontal
813 and posterior temporal cortex. *Neuropsychologia*, *76*, 92–107.

https://doi.org/10.1016/j.neuropsychologia.2015.02.030

Krieger-Redwood, K., Jefferies, E., Karapanagiotidis, T., Seymour, R., Nunes, A., Ang, J. W. A., ... & Smallwood, J. (2016). Down but not out in posterior cingulate cortex: Deactivation yet functional coupling with prefrontal cortex during demanding semantic cognition. *Neuroimage*, *141*, 366-377. https://doi.org/10.1016/j.neuroimage.2016.07.060

Lambon Ralph, M. A., Jefferies, E., Patterson, K., & Rogers, T. T. (2016). The neural and computational bases of semantic cognition. *Nature Reviews Neuroscience*. https://doi.org/10.1038/nrn.2016.150

Langner, O., Dotsch, R., Bijlstra, G., Wigboldus, D. H. J., Hawk, S. T., & van Knippenberg, A. (2010). Presentation and validation of the Radboud Faces Database. *Cognition and Emotion*, *24*(8), 1377–1388. https://doi.org/10.1080/02699930903485076

Lanzoni, L., Thompson, H., Beintari, D., Berwick, K., Demnitz-King, H., Raspin, H., … Jefferies, E. (2019). Emotion and location cues bias conceptual retrieval in people with deficient semantic control. *Neuropsychologia*, *131*(June), 294–305. https://doi.org/10.1016/j.neuropsychologia.2019.05.030

Leech, R., & Sharp, D. J. (2014). The role of the posterior cingulate cortex in cognition and disease. *Brain*, *137*(1), 12–32. https://doi.org/10.1093/brain/awt162

Margulies, D. S., Ghosh, S. S., Goulas, A., Falkiewicz, M., Huntenburg, J. M., Langs, G., … Smallwood, J. (2016). Situating the default-mode network along a principal gradient of macroscale cortical organization. *Proceedings of the National Academy of Sciences of the United States of America*, *113*(44), 12574–12579. https://doi.org/10.1073/pnas.1608282113

Mesulam, M. M. (1998). From sensation to cognition. *Brain*, *121*(6), 1013–1052. https://doi.org/10.1093/brain/121.6.1013

Mollo, G., Cornelissen, P. L., Millman, R. E., Ellis, A. W., & Jefferies, E. (2017). Oscillatory dynamics supporting semantic cognition: Meg evidence for the contribution of the anterior temporal lobe hub and modality-specific spokes. *PLoS ONE*, *12*(1), 1–25. https://doi.org/10.1371/journal.pone.0169269

Murphy, C., Jefferies, E., Rueschemeyer, S. A., Sormaz, M., Wang, H. ting, Margulies, D. S., & Smallwood, J. (2018). Distant from input: Evidence of regions within the default mode network supporting perceptually-decoupled and conceptually-guided cognition. *NeuroImage*, *171*(January), 393–401. https://doi.org/10.1016/j.neuroimage.2018.01.017

Murphy, C., Wang, H. T., Konu, D., Lowndes, R., Margulies, D. S., Jefferies, E., & Smallwood, J. (2019). Modes of operation: A topographic neural gradient supporting stimulus dependent and independent cognition. *NeuroImage*, *186*(November 2018), 487–496. https://doi.org/10.1016/j.neuroimage.2018.11.009

Murphy, K., Birn, R. M., Handwerker, D. A., Jones, T. B., & Bandettini, P. A. (2009). The impact of global signal regression on resting state correlations: Are anti-correlated networks introduced? *NeuroImage*, *44*(3), 893–905. https://doi.org/10.1016/j.neuroimage.2008.09.036

Naghavi, H. R., & Nyberg, L. (2005). Common fronto-parietal activity in attention, memory, and consciousness: shared demands on integration?. *Consciousness and cognition*, *14*(2), 390-425. https://doi.org/10.1016/j.concog.2004.10.003

Noonan, K. a, Jefferies, E., Corbett, F., & Lambon Ralph, M. a. (2010). Elucidating the nature of deregulated semantic cognition in semantic aphasia: evidence for the roles of prefrontal and temporo-parietal cortices. *Journal of Cognitive Neuroscience*, *22*(7), 1597–1613. https://doi.org/10.1162/jocn.2009.21289

Noonan, K. a, Jefferies, E., Visser, M., & Lambon Ralph, M. a. (2013). Going beyond Inferior Prefrontal Involvement in Semantic Control: Evidence for the Additional Contribution of Dorsal Angular Gyrus and Posterior Middle Temporal Cortex. *Journal of Cognitive Neuroscience*, 1–10. https://doi.org/10.1162/jocn

Owen, A. M., McMillan, K. M., Laird, A. R., & Bullmore, E. (2005). N-back working memory paradigm: A meta-analysis of normative functional neuroimaging studies. *Human brain mapping*, *25*(1), 46-59. https://doi.org/10.1002/hbm.20131

Patterson, K., Nestor, P. J., & Rogers, T. T. (2007). Where do you know what you know? The representation of semantic knowledge in the human brain. *Nature Reviews.*

Neuroscience, *8*(december), 976–987. https://doi.org/10.1038/nrn2277

Price, Amy R, Bonner, M. F., Peelle, J. E., & Grossman, M. (2015). Converging evidence for the neuroanatomic basis of combinatorial semantics in the angular gyrus. *The Journal of Neuroscience : The Official Journal of the Society for Neuroscience*, *35*(7), 3276–3284. https://doi.org/10.1523/JNEUROSCI.3446-14.2015

Price, Amy Rose, Peelle, J. E., Bonner, M. F., Grossman, M., & Hamilton, R. H. (2016). Causal evidence for a mechanism of semantic integration in the angular Gyrus as revealed by high-definition transcranial direct current stimulation. *Journal of Neuroscience*, *36*(13), 3829–3838. https://doi.org/10.1523/JNEUROSCI.3120-15.2016

Pylkkänen, L. (2019). The neural basis of combinatory syntax and semantics. *Science*, *366*(6461), 62–66. https://doi.org/10.1126/science.aax0050

Raichle, M. E., MacLeod, A. M., Snyder, A. Z., Powers, W. J., Gusnard, D. A., & Shulman, G. L. (2001). A default mode of brain function. *Proceedings of the National Academy of Sciences of the United States of America*, *98*(2), 676–682. https://doi.org/10.1073/pnas.98.2.676

Ramanan, S., Piguet, O., & Irish, M. (2017). Rethinking the Role of the Angular Gyrus in Remembering the Past and Imagining the Future: The Contextual Integration Model. *The Neuroscientist*, 107385841773551. https://doi.org/10.1177/1073858417735514

Robin, J., Buchsbaum, B. R., & Moscovitch, M. (2018). The primacy of spatial context in the neural representation of events. *The Journal of Neuroscience*, *38*(11), 1638–17. https://doi.org/10.1523/JNEUROSCI.1638-17.2018

Rodd, J. M., Cai, Z. G., Betts, H. N., Hanby, B., Hutchinson, C., & Adler, A. (2016). The impact of recent and long-term experience on access to word meanings: Evidence from large-scale internet-based experiments. *Journal of Memory and Language*, *87*, 16–37. https://doi.org/10.1016/j.jml.2015.10.006

Rodd, J. M., Davis, M. H., & Johnsrude, I. S. (2005). The neural mechanisms of speech comprehension: fMRI studies of semantic ambiguity. *Cerebral Cortex*, *15*(8), 1261–1269. https://doi.org/10.1093/cercor/bhi009

900 Rodd, J. M., Gaskell, M. G., & Marslen-Wilson, W. D. (2004). Modelling the effects of semantic
901 ambiguity in word recognition. *Cognitive Science*, *28*(1), 89–104.
902 https://doi.org/10.1016/j.cogsci.2003.08.002

903 Rodd, J. M., Lopez Cutrin, B., Kirsch, H., Millar, A., & Davis, M. H. (2013). Long-term priming of
904 the meanings of ambiguous words. *Journal of Memory and Language*, *68*(2), 180–198.
905 https://doi.org/10.1016/j.jml.2012.08.002

906 Seghier, M. L., Lazeyras, F., Pegna, A. J., Annoni, J. M., Zimine, I., Mayer, E., ... & Khateb, A.
907 (2004). Variability of fMRI activation during a phonological and semantic language task
908 in healthy subjects. *Human brain mapping*, *23*(3), 140-155.
909 https://doi.org/10.1002/hbm.20053

910 Seghier, M. L., Fagan, E., & Price, C. J. (2010). Functional subdivisions in the left angular gyrus
911 where the semantic system meets and diverges from the default network. *Journal of*
912 *Neuroscience*, *30*(50), 16809–16817. https://doi.org/10.1523/JNEUROSCI.3377-10.2010

913 Simpson, J. R., Öngür, D., Akbudak, E., Conturo, T. E., Ollinger, J. M., Snyder, A. Z., … Raichle,
914 M. E. (2000). The emotional modulation of cognitive processing: An fMRI study. *Journal*
915 *of Cognitive Neuroscience*, *12*(SUPPL. 2), 157–170.
916 https://doi.org/10.1162/089892900564019

917 Smallwood, J. (2013). Distinguishing how from why the mind wanders: A process-occurrence
918 framework for self-generated mental activity. *Psychological Bulletin*, *139*(3), 519–535.
919 https://doi.org/10.1037/a0030010

920 Smith, S. M. (2002). Fast robust automated brain extraction. *Human Brain Mapping*, *17*(3),
921 143–155. https://doi.org/10.1002/hbm.10062

922 Teige, C., Cornelissen, P. L., Mollo, G., Gonzalez Alam, T. R. del J., McCarty, K., Smallwood, J.,
923 & Jefferies, E. (2019). Dissociations in semantic cognition: Oscillatory evidence for
924 opposing effects of semantic control and type of semantic relation in anterior and
925 posterior temporal cortex. *Cortex*, *120*, 308–325.
926 https://doi.org/10.1016/j.cortex.2019.07.002

927 Teige, C., Mollo, G., Millman, R., Savill, N., Smallwood, J., Cornelissen, P. L., & Jefferies, E.
928 (2018). Dynamic semantic cognition: Characterising coherent and controlled conceptual

retrieval through time using magnetoencephalography and chronometric transcranial magnetic stimulation. *Cortex*, *103*, 329–349. https://doi.org/10.1016/j.cortex.2018.03.024

Townsend, J. T., & Ashby, F. G. (1983). Stochastic Modeling of Elementary Psychological Processes. *The American Journal of Psychology*, *98*(3), 480. https://doi.org/10.2307/1422636

Twilley, L. C., Dixon, P., Taylor, D., & Clark, K. (1994). University of Alberta norms of relative meaning frequency for 566 homographs. *Memory & Cognition*, *22*(1), 111–126. https://doi.org/10.3758/BF03202766

van Heuven, W. J., Mandera, P., Keuleers, E., & Brysbaert, M. (2014). SUBTLEX-UK: A new and improved word frequency database for British English. The Quarterly Journal of Experimental Psychology, 67(6), 1176-1190. https://doi.org/10.1080/17470218.2013.850521

Vatansever, D., Manktelow, A. E., Sahakian, B. J., Menon, D. K., & Stamatakis, E. A. (2017). Angular default mode network connectivity across working memory load. *Human Brain Mapping*, *38*(1), 41–52. https://doi.org/10.1002/hbm.23341

Vatansever, Deniz, Menon, X. D. K., Manktelow, A. E., Sahakian, B. J., & Stamatakis, E. A. (2015). Default Mode Dynamics for Global Functional Integration. *The Journal of Neuroscience : The Official Journal of the Society for Neuroscience*, *35*(46), 15254–15262. https://doi.org/10.1523/JNEUROSCI.2135-15.2015

Vitello, S., & Rodd, J. M. (2015). Resolving Semantic Ambiguities in Sentences: Cognitive Processes and Brain Mechanisms. *Linguistics and Language Compass*, *9*(10), 391–405. https://doi.org/10.1111/lnc3.12160

Whitfield-Gabrieli, S., & Nieto-Castanon, A. (2012). Conn: A Functional Connectivity Toolbox for Correlated and Anticorrelated Brain Networks. *Brain Connectivity*, *2*(3), 125–141. https://doi.org/10.1089/brain.2012.0073

Whitney, C., Kirk, M., O'Sullivan, J., Lambon Ralph, M. a., & Jefferies, E. (2011). The neural organization of semantic control: TMS evidence for a distributed network in left inferior frontal and posterior middle temporal gyrus. *Cerebral Cortex*, *21*(5), 1066–1075.

https://doi.org/10.1093/cercor/bhq180

Willenbockel, V., Sadr, J., Fiset, D., Horne, G. O., Gosselin, F., & Tanaka, J. W. (2010). Controlling low-level image properties: The SHINE toolbox. *Behavior Research Methods*, *42*(3), 671–684. https://doi.org/10.3758/BRM.42.3.671

Woolgar, A., Hampshire, A., Thompson, R., & Duncan, J. (2011). Adaptive coding of task-relevant information in human frontoparietal cortex. *Journal of Neuroscience*, *31*(41), 14592–14599. https://doi.org/10.1523/JNEUROSCI.2616-11.2011

Woolrich, M. (2008). Robust group analysis using outlier inference. *NeuroImage*, *41*(2), 286–301. https://doi.org/10.1016/j.neuroimage.2008.02.042

Woolrich, M. W., Behrens, T. E. J., Beckmann, C. F., Jenkinson, M., & Smith, S. M. (2004). Multilevel linear modelling for FMRI group analysis using Bayesian inference. *NeuroImage*, *21*(4), 1732–1747. https://doi.org/10.1016/j.neuroimage.2003.12.023

Woolrich, M. W., Ripley, B. D., Brady, M., & Smith, S. M. (2001). Temporal autocorrelation in univariate linear modeling of FMRI data. *NeuroImage*, *14*(6), 1370–1386. https://doi.org/10.1006/nimg.2001.0931

Worsley, K.J. Statistical analysis of activation images. Ch 14, in Functional MRI: An Introduction to Methods, eds. P. Jezzard, P.M. Matthews and S.M. Smith. OUP, 2001.

Xia, M., Wang, J., & He, Y. (2013). BrainNet Viewer: A Network Visualization Tool for Human Brain Connectomics. *PLoS ONE*, *8*(7). https://doi.org/10.1371/journal.pone.0068910

Yarkoni, T., Poldrack, R. A., Nichols, T. E., Van Essen, D. C., & Wager, T. D. (2011). Large-scale automated synthesis of human functional neuroimaging data. *Nature Methods*, *8*(8), 665–670. https://doi.org/10.1038/nmeth.1635

Yeo, B. T. T., Krienen, F. M., Sepulcre, J., Sabuncu, M. R., Lashkari, D., Hollinshead, M., … Buckner, R. L. (2011). The organization of the human cerebral cortex estimated by intrinsic functional connectivity. *Journal of Neurophysiology*, *106*, 1125–1165. https://doi.org/10.1152/jn.00338.2011.

SUPPLEMENTARY MATERIAL

Group behavioural performance

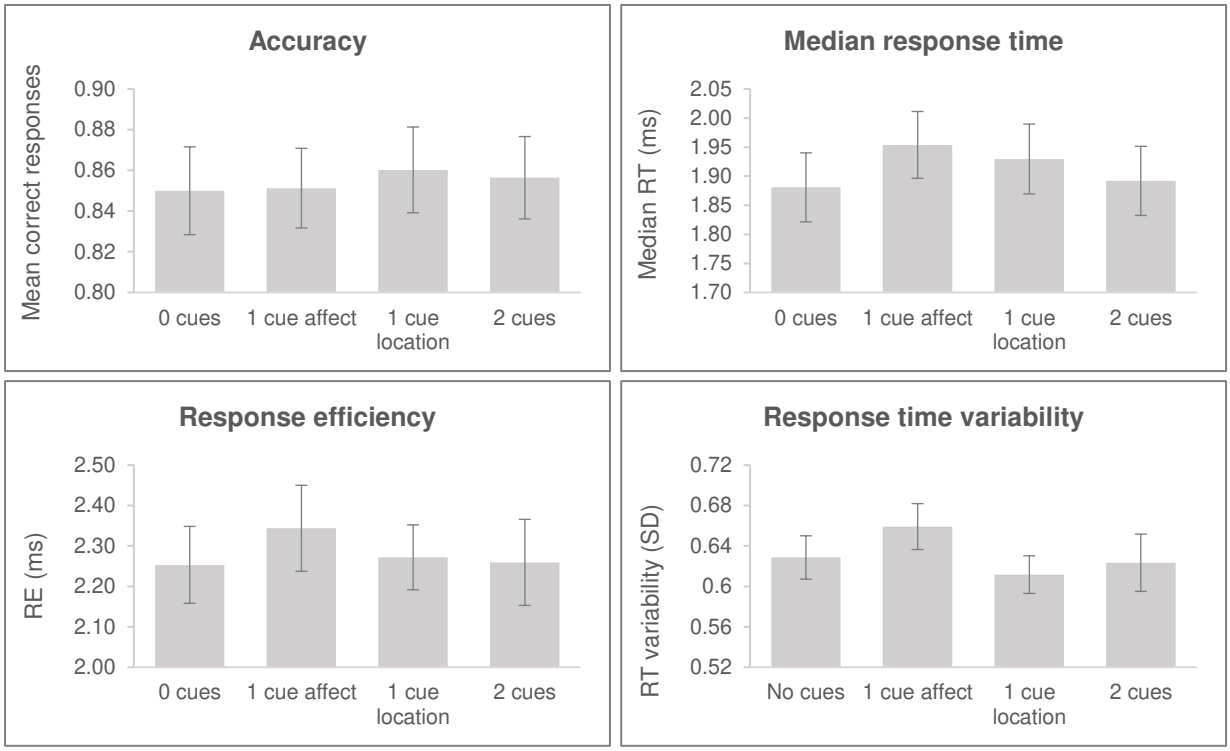

Figure S1. Accuracy (mean correct responses), median RT for correct trials (milliseconds), response efficiency scores (median RT/mean correct responses), and RT variability (mean standard deviation per participant per condition) do not differ significantly across conditions. Error bars show standard error of the mean (SEM).

	Summary statistics			
	Accuracy	Median RT	Response efficiency	RT variability
0 cues	0.85 (0.11)	1.88 (0.30)	2.25 (0.49)	0.63 (0.11)
1 cue affect	0.85 (0.10)	1.95 (0.29)	2.34 (0.54)	0.66 (0.12)
1 cue location	0.86 (0.11)	1.93 (0.31)	2.27 (0.41)	0.61 (0.10)
2 cues	0.86 (0.10)	1.89 (0.30)	2.26 (0.54)	0.62 (0.14)

Table S1. Descriptive statistics for the cueing task. Mean and (standard deviation) values are provided.

Supplementary behavioural analyses

1- way repeated measures ANOVAs on cue condition

	Accuracy	Median RT	Response efficiency	RT variability
F	0.14	0.95	0.62	1.26
df	3, 75	3, 75	3, 75	3, 75
p	0.939	0.420	0.605	0.296
partial η2	0.01	0.04	0.02	0.05

Table S2. Behavioural performance did not differ significantly across cue conditions, as revealed by 1-way ANOVAs on accuracy, median response time, response efficiency, and response time variability.

Univariate contrasts of activation during cue presentation

Below we report the group-level statistical maps ($z > 3.1$) for the cue model. In this model we looked at changes in the BOLD response in response to the presentation of the visual cues. Semantic decisions (which happen subsequently to the presentation of cues) were modelled separately; the statistical maps that survived the threshold of $z > 3.1$ can be seen in the body of the manuscript (Figure 2B and 4).

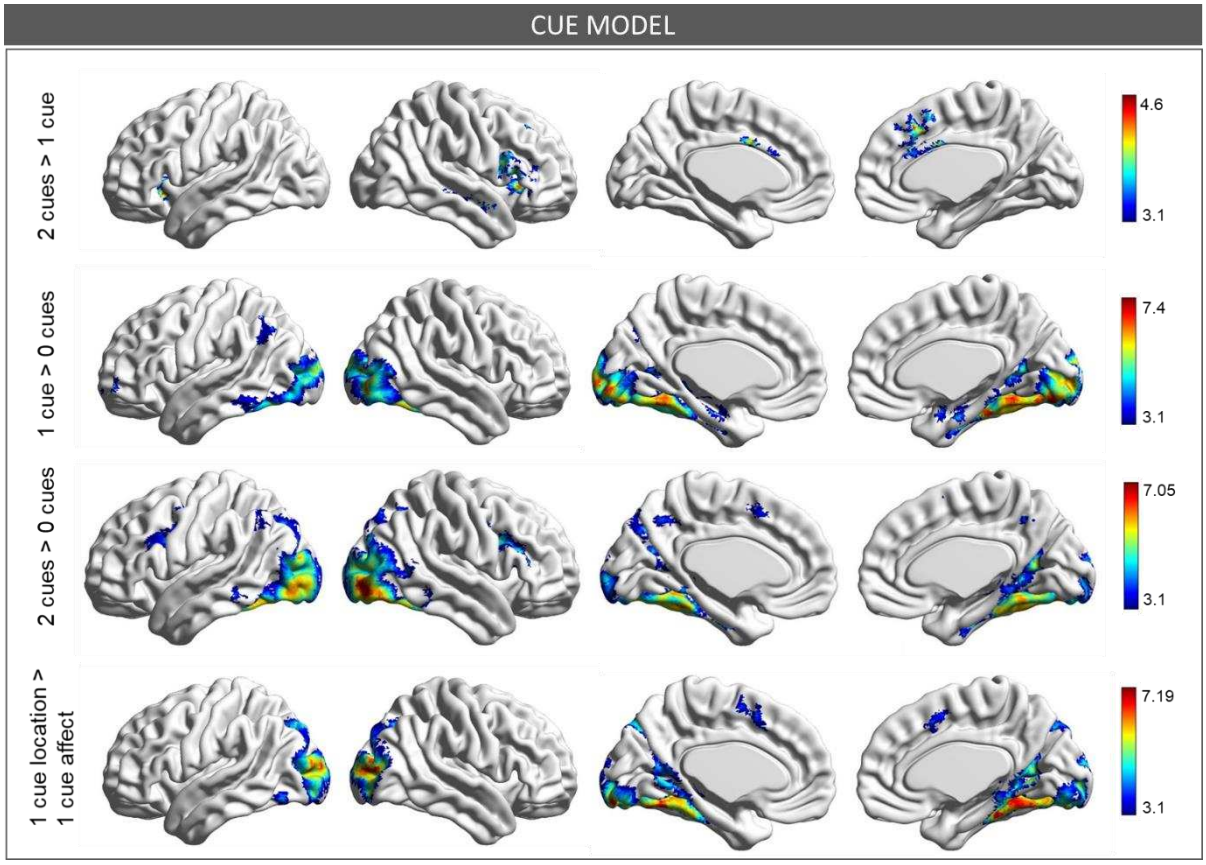

Figure S2. Univariate results for the cue model (i.e. when the cues were presented, prior to the semantic decision). From top to bottom: 2 cues > 1 cue (processing of 2 cues > 1 cue [average of affect and location]), 1 cue > 0 cues (processing of 1 cue [average of affect and location] > 0 cues [scrambled images]); 2 cues > 0 cues; 1 cue location > 1 cue affect. The reverse contrast (1 cue affect > 1 cue location) yielded no clusters. Coordinates of cluster peaks for these comparisons are reported in Table S3.

Basic effect of semantic decisions

In the main manuscript we defined the semantic regions recruited during the task using a contrast of 0 cues > letter strings (Figure 2A). Below we report the contrasts of each of the other task conditions against the presentation of letter strings (i.e. non semantic task).

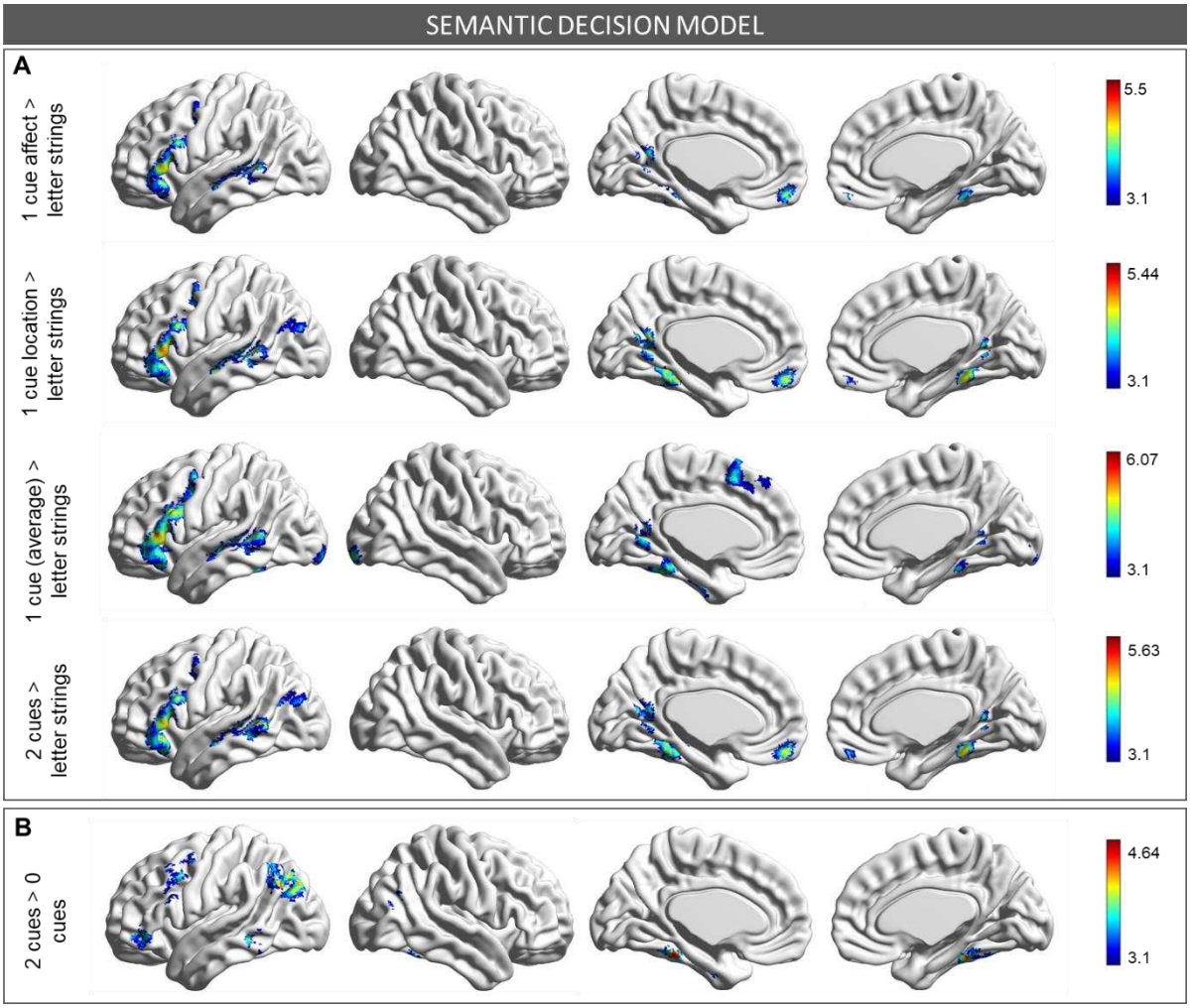

Figure S3. A. Basic effect of semantic decisions as estimated by contrasts of the task conditions > letter strings (i.e. non-semantic task). These univariate contrasts for the semantic decision model (i.e. when participants were making decisions following the presentation of 0, 1, 2 cues) reveal a similar pattern of activation. B. Semantic decisions following 2 cues vs. 0 cues.

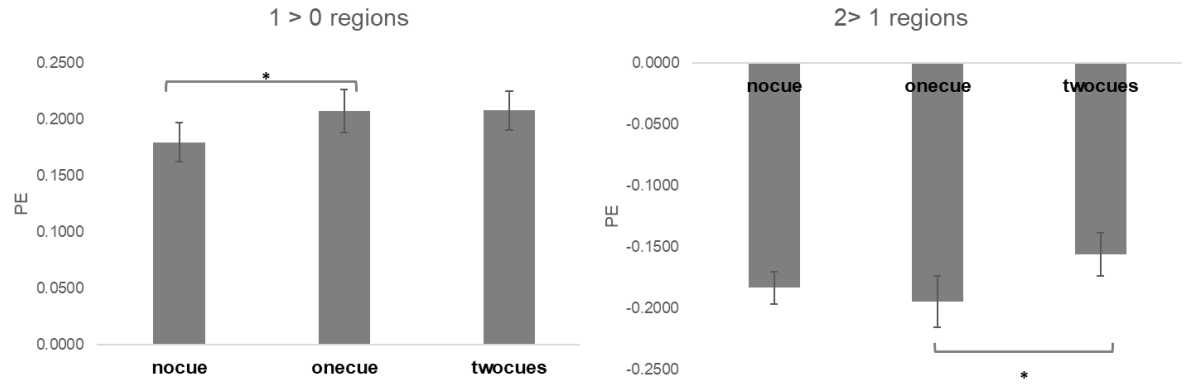

Figure S4. ROI analysis extracting the parameter estimates (PE) for the three conditions over the implicit baseline at the time of making semantic decisions (semantic decision model) in the 1 > 0 and 2 > 1 maps. We ran two repeated measures ANOVAs that found that the recruitment is different across cueing conditions in both 1 > 0 [$F(2,50) = 3.36$, $p = .043$, $\eta^2 = .12$] and 2 > 1 [$F(2,50) = 3.47$, $p = .039$, $\eta^2 = .12$] regions. Bonferroni-corrected pairwise comparisons revealed reduced activation for 0 cue condition compared to 1 cue in 1 > 0 regions [$t(25) = -2.59$, $p = .016$], and reduced de-activation in 2 cues compared to 1 cue in 2 > 1 regions [$t(25) = -3.03$, $p = .006$].

Peak co-ordinates for clusters identified by the cue model and the semantic decision model

Contrast	Region	Voxels	Z-score	MNI coordinates (x, y, z)		
	Cue model					
2 + 1 > 0	R. Lingual gyrus, occipital fusiform gyrus, occipital pole	26628	7.49	8	-82	-12
	L. Middle frontal gyrus, superior frontal gyrus	769	4.51	-36	22	54
	L. Frontal pole	766	4.99	-42	54	-4
	L. temporal pole, inferior temporal gyrus (anterior), temporal fusiform gyrus (anterior)	130	4.29	-42	4	-42
2 > 0	R. Lateral occipital cortex (inferior), occipital pole	21099	7.05	42	-86	-8
	R. Precentral gyrus, inferior frontal gyrus, middle frontal gyrus	866	5.11	38	10	28
	L. Inferior frontal gyrus (pars opercularis), precentral gyrus, middle frontal gyrus	850	4.63	-40	16	22
	Bilateral precuneus	189	4.11	0	-56	46
	L. Supplementary motor cortex, paracingulate gyrus, superior frontal gyrus	177	4.29	-4	6	54
2 > 1	R. Frontal operculum cortex, inferior frontal gyrus (pars opercularis), inferior frontal gyrus (pars triangularis)	940	4.48	46	18	6
	R. Paracingulate gyrus, superior frontal gyrus, cingulate gyrus (anterior)	585	4.38	6	24	44
	R. Middle frontal gyrus, superior frontal gyrus, frontal pole	267	4.55	28	32	44
	R. Superior temporal gyrus (anterior), middle temporal gyrus (anterior), superior temporal gyrus (posterior), middle temporal gyrus (posterior)	199	4.35	54	-6	-16
	L. Insular cortex	152	4.51	-28	20	-6
1 > 0	R. Occipital fusiform gyrus, lingual gyrus	21130	7.38	24	-72	-14
	L. Lateral occipital cortex (superior), angular gyrus	229	4	-50	-66	40
	L. Frontal pole	229	4.51	-40	58	2
	R. Cerebellum	198	4.24	28	-74	-44
1 location > 1 affect	R. Occipital pole, lateral occipital cortex	17891	7.19	36	-88	8
	Bilateral paracingulate gyrus, supplementary motor cortex	411	4.31	0	10	50
	Semantic decision model					
0 > letter strings	L. Inferior frontal gyrus (pars triangularis), frontal pole, middle frontal gyrus	1672	5.92	-54	32	8

	L. Superior temporal gyrus (posterior), middle temporal gyrus (posterior), supramarginal gyrus (posterior)	953	5.52	-56	-42	4
	R. Cerebellum	644	5.04	10	-82	-36
	L. Temporal fusiform cortex (posterior), parahippocampal gyrus (posterior), inferior temporal gyrus (posterior)	400	4.51	-38	-30	-18
	L. Cerebellum	280	4.62	-8	-60	14
	L. Frontal medial cortex, frontal pole	256	4.66	-4	52	-16
	R. Temporal occipital fusiform, Lingual gyrus, parahippocampal gyrus (posterior)	220	4.91	22	-42	-16
	L. Precentral gyrus, middle frontal gyrus	153	4.7	-38	0	46
1 affect > letter strings	L. Inferior frontal gyrus (pars triangularis), frontal pole, middle frontal gyrus	1684	4.91	-56	32	6
	L. Middle temporal gyrus (temporo-occipital part), middle temporal gyrus (posterior)	926	5.5	-56	-44	4
	R. Cerebellum	571	4.81	10	-82	-36
	L. Temporal fusiform (posterior), parahippocampal gyrus (posterior), inferior temporal gyrus (posterior)	261	4.2	-38	-30	-18
	L. Precuneus, intracalcarine cortex, supracalcarine cortex, cingulate gyrus (posterior)	258	4.65	-8	-60	14
	L. Medial frontal cortex, frontal pole	186	4.6	-2	52	-16
	R. Temporal fusiform (posterior), parahippocampal gyrus (posterior), lingual gyrus	138	4.19	24	-38	-18
	L. Precentral gyrus, middle frontal gyrus	125	4.11	-38	0	44
1 location > letter strings	L. Inferior frontal gyrus (pars triangularis), frontal pole, middle frontal gyrus	2000	5.44	-56	32	8
	L. Middle temporal gyrus (temporo-occipital part), middle temporal gyrus (posterior)	1107	5.04	-58	-44	4
	R. Cerebellum	910	5.12	12	-78	-30
	L. Temporal fusiform (posterior), parahippocampal gyrus (posterior), inferior temporal gyrus (posterior)	773	5.06	-38	-30	-18
	L. Precuneus, intracalcarine cortex, lingual gyrus, supracalcarine cortex, cingulate gyrus (posterior)	723	4.93	-8	-60	10
	R. Lingual gyrus, occipital fusiform gyrus, parahippocampal gyrus (posterior), temporal fusiform (posterior)	375	5.4	20	-40	-16
	L. Medial frontal cortex, frontal pole	230	4.71	-2	52	-16
	L. Precentral gyrus, middle frontal gyrus	205	4.61	-38	0	44
	L. Lateral occipital cortex (superior)	176	3.97	-44	-84	26
1 > letter strings	L. Inferior frontal gyrus (pars triangularis), frontal pole, middle frontal gyrus	3459	5.65	-54	30	8
	L. Middle temporal gyrus (temporo-occipital part), middle temporal gyrus (posterior)	2493	5.41	-56	-44	4
	R. Cerebellum	1165	6.07	12	-78	-28
	L. Precuneus, lingual gyrus, intracalcarine cortex, cingulate gyrus (posterior), supracalcarine cortex	371	4.73	-6	-58	8
	L. Paracingulate gyrus, superior frontal gyrus, juxtapositional lobule	337	4.56	-6	14	52
	R. Occipital pole	275	4.89	18	-100	-12

	L. Occipital pole	235	4.91	-34	-98	-14
	R. Precuneus, lingual gyrus, intracalcarine cortex, cingulate gyrus (posterior), supracalcarine cortex	127	4.54	14	-56	6
	R. temporal fusiform (posterior), parahippocampal gyrus (posterior), lingual gyrus	118	4.37	28	-36	-20
2 > letter strings	L. Inferior frontal gyrus (pars triangularis), frontal pole, middle frontal gyrus	2239	5.51	-56	32	8
	L. Middle temporal gyrus (temporo-occipital), middle temporal gyrus (posterior), supra-marginal gyrus (posterior), , superior temporal gyrus (posterior)	1175	5.63	-48	-44	-2
	R. Cerebellum	794	4.79	10	-82	-34
	L. Temporal fusiform (posterior), temporal occipital fusiform, parahippocampal gyrus (posterior), lingual gyrus	695	4.95	-26	-42	-20
	L. Precuneus, lingual gyrus, intracalcarine cortex, cingulate gyrus (posterior), supracalcarine cortex	458	4.77	-8	-58	10
	R. Temporal occipital fusiform, Lingual gyrus, temporal fusiform (posterior), parahippocampal gyrus (posterior)	367	5.6	22	-40	-16
	L. Angular gyrus, lateral occipital cortex (superior), lateral occipital cortex (inferior)	265	4.4	-40	-60	18
	L. Frontal medial cortex, frontal pole	237	4.82	-2	52	-16
	R. Precuneus, Intracalcarine cortex, cingulate gyrus (posterior), lingual gyrus, supracalcarine cortex	201	4.67	16	-54	8
2 > 1	R. Lateral occipital cortex (superior)	5247	5.94	52	-70	30
	R. Frontal pole, paracingulate gyrus, frontal medial cortex	4395	5.57	4	56	0
	L. lateral occipital cortex (superior), angular gyrus, supramarginal gyrus (posterior)	1639	5.27	-50	-62	42
	R. Precuneus, cingulate gyrus (posterior)	1521	5.17	8	-56	26
	L. Cerebellum	745	4.77	-26	-78	-36
	L. Middle frontal gyrus	304	4.46	-36	26	42
	R. Frontal pole	191	4.35	40	48	-10
	L. Frontal pole	172	4.33	-30	62	-2
	R. Temporo-occipital fusiform, lingual gyrus, parahippocampal gyrus	143	4.72	24	-42	-16
1 > 0	R. Cerebellum	30503	6.81	4	-74	-28
	L. Supplementary motor cortex, paracingulate gyrus, superior frontal gyrus, cingulate gyrus (anterior)	2167	6.57	-4	8	52
	R. Inferior frontal gyrus (pars opercularis), middle frontal gyrus, inferior frontal gyrus (pars triangularis), precentral gyrus	714	5.59	42	22	20
	L. Middle temporal gyrus (temporo-occipital), supra-marginal gyrus (posterior), middle temporal gyrus (posterior), superior temporal gyrus	254	4.85	-56	-46	4
2 > 0	L. Lateral occipital cortex (superior), angular gyrus	1431	4.55	-46	-66	32
	R. Lateral occipital cortex (inferior), occipital fusiform gyrus	533	4.55	38	-74	-24
	L. Middle frontal gyrus, precentral gyrus, inferior frontal gyrus (pars opercularis)	472	4.04	-46	12	40

L. Temporal fusiform cortex (posterior), temporal occipital fusiform cortex, parahippocampal gyrus (posterior)	441	4.64	-26	-40	-20
L. Occipital fusiform gyrus	283	4.55	-46	-72	-26
L. Frontal pole, frontal orbital cortex, inferior frontal gyrus (pars triangularis)	153	3.94	-52	40	-8
L. Middle temporal gyrus (posterior), middle temporal gyrus (temporooccipital)	128	3.97	-60	-40	-8
R. Lateral occipital cortex (superior), angular gyrus	125	3.94	52	-64	24

Table S3. Coordinates of cluster peaks for the main contrasts of interest. From top to bottom: cue model – 2 + 1 > 0 (processing of cues > scrambles images), 2 > 0 (processing of 2 cues [affect and location] > 0 cues [scrambled images]), 2 > 1 (processing of 2 cues [affect and location] > 1 cue [average of affect and location]), 1 > 0 (processing of 1 cue [average of affect and location] > 0 cues [scrambled images]), 1 affect > 1 location; semantic decision model - 0 cues > letter strings (semantic decisions in the absence of a semantic cue > non semantic decisions in the absence of cues), 1 affect > letter strings, 1 location > letter strings, 1 > letter strings (semantic decision following 1 cue [average of affect and location] > non semantic decisions in the absence of cues), 2 > letter strings, 2 > 1 (semantic decisions following multiple cues > semantic decisions following 1 cue), 1 > 0 (semantic decisions following 1 semantic cue > semantic decisions in the absence of a semantic cue). The location of the peaks is labelled according to the Harvard-Oxford Structural Cortical Atlas tool available in FSL. Caption: R = right hemisphere, L = left hemisphere, cluster corrected at z > 3.1.

Supplementary analyses examining activation for the semantic task along the Principal Gradient

2 (cue contrast: 2 vs. 1, 1 vs. 0) x 10 (gradient bin: bin1 - bin10) ANOVA

	Test of within-subjects effect			Test of within-subjects contrasts			
	Cue contrast	Gradient bin	Cue contrast x gradient bin	Cue contrast	Gradient bin	Cue contrast x gradient bin	
F	0.33	1.82	28.33	0.33	1.53	37.27	Linear
p	.571	.164	<.001*	.571	.227	<.001*	
partial η^2	0.01	0.07	0.53	0.01	0.06	0.60	
F					0.06	12.37	Quadratic
p					.815	.002*	
partial η^2					0.00	0.33	
F					2.26	6.47	Cubic
p					.145	.018*	
partial η^2					0.08	0.21	
F					0.79	0.28	Order 4
p					.382	.601	
partial η^2					0.03	0.01	
F					20.44	111.60	Order 5
p					<.001*	<.001*	
partial η^2					0.45	0.82	
F					1.06	9.51	Order 6
p					.312	.005*	
partial η^2					0.04	0.28	
F					5.07	38.85	Order 7
p					.033*	<.001*	
partial η^2					0.17	0.61	
F					2.50	64.54	Order 8
p					.127	<.001*	
partial η^2					0.09	0.72	
F					1.07	66.73	Order 9
p					.311	<.001*	
partial η^2					0.04	0.73	

Table S4. Values for the 2-way repeated measure ANOVA on cue contrast (2 levels: 2 cues > 1 cue; 1 cue > 0 cues) and gradient bin (10 levels: bin1 – bin10). Degrees of freedom for the Test of Within-subjects Effects: cue condition [1, 25]; gradient bin [2.37, 59.16]; cue contrast x gradient bin [2.04, 51.01]. Degrees of freedom for the Test of Within-subjects Contrasts: cue contrast, gradient bin, cue contrast x gradient bin [1, 25]. Significant results and interactions are marked with *. A Greenhouse-Geisser correction was applied where the assumption of sphericity was not met.

1 way RM ANOVA on 2 cues > 1 cue along the gradient

	Test of within-subjects effect	Test of within-subjects contrasts	
	Gradient bin	Gradient bin	
F	31.50	47.13	Linear
p	<.001*	<.001*	
partial η^2	0.56	0.65	
F		11.38	Quadratic
p		.002*	
partial η^2		0.31	
F		3.03	Cubic
p		.094	
partial η^2		0.11	
F		0.06	Order 4
p		.813	
partial η^2		0.00	
F		70.22	Order 5
p		<.001*	
partial η^2		0.74	
F		7.66	Order 6
p		.010*	
partial η^2		0.23	
F		31.30	Order 7
p		<.001*	
partial η^2		0.56	
F		48.60	Order 8
p		<.001*	
partial η^2		0.66	
F		50.58	Order 9
p		<.001*	
partial η^2		0.67	

Table S5. Values for the 1-way repeated measure ANOVA on the parameter estimates for the univariate contrast of 2 cues > 1 cue extracted along the gradient (10 levels: bin1 – bin10). Degrees of freedom for the Test of Within-subjects Effects: 2.13, 53.30. Degrees of freedom for the Test of Within-subjects Contrasts: 1, 25. Significant results and interactions are marked with *. A Greenhouse-Geisser correction was applied where the assumption of sphericity was not met.

1 way RM ANOVA on 1 cue > 0 cues along the gradient

	Test of within-subjects effect	Test of within-subjects contrasts	
	Gradient bin	Gradient bin	
F	21.37	24.80	Linear
p	<.001*	<.001*	
partial η^2	0.46	0.50	
F		11.48	Quadratic
p		.002*	
partial η^2		0.31	
F		7.44	Cubic
p		.011*	
partial η^2		0.23	
F		0.52	Order 4
p		.478	
partial η^2		0.02	
F		116.31	Order 5
p		<.001*	
partial η^2		0.82	
F		8.61	Order 6
p		.007*	
partial η^2		0.26	
F		40.27	Order 7
p		<.001*	
partial η^2		0.62	
F		62.44	Order 8
p		<.001*	
partial η^2		0.71	
F		64.32	Order 9
p		<.001*	
partial η^2		0.72	

Table S6. Values for the 1-way repeated measure ANOVA on the parameter estimates for the univariate contrast of 1 cue > 0 cues extracted along the gradient (10 levels: bin1 – bin10). Degrees of freedom for the Test of Within-subjects Effects: 2.05, 51.22. Degrees of freedom for the Test of Within-subjects Contrasts: 1, 25. Significant results and interactions are marked with *. A Greenhouse-Geisser correction was applied where the assumption of sphericity was not met.

Analysis of intrinsic connectivity

As there is evidence that DMN is anti-correlated with task-positive regions captured by MDN (Blank et al., 2014; Davey et al., 2016; Fox et al., 2005), we predicted that our contrast maps of 1 > 0 and 2>1 should fall within regions with distinct patterns of intrinsic connectivity at rest, given their spatial similarity with the MDN and with the DMN, respectively.

Materials and Methods

Participants

Whole-brain intrinsic connectivity maps for the two contrasts (1 >0 and 2>1) were produced using a sample of 86 participants recruited as part of a different study. The study was approved by the Ethics Committees of the York Neuroimaging Centre and the Department of Psychology, University of York. Volunteers provided written consent and were debriefed after the experiment.

MRI data acquisition

Structural and functional MRI data were acquired using a 3T GE HDx Excite MRI scanner at the York Neuroimaging Centre, University of York. Structural MRI acquisition was based on the same protocol used for the main sample of this experiment (see Materials and Methods– *fMRI acquisition*). Resting-state fMRI data was recorded from the whole brain using single-shot 2D gradient-echo-planar imaging (TR=3s, TE=minimum full, flip angle=90°, matrix size=64x64, 60 slices, voxel size=3x3x3mm3, 180 volumes). Participants were asked to passively view a fixation cross and not to think of anything in particular for the duration of the resting-state scan (9 minutes). A T1 weighted FLAIR scan with the same orientation as the functional scans was collected to improve co-registration between subject-specific structural and functional scans (TR=2560ms, TE=minimum full, matrix size=64x64, voxel size=3x3x3mm3).

Pre-processing

The pre-processing of resting state data was performed using the CONN functional connectivity toolbox V.18a (http://www.nitrc.org/projects/conn; Whitfield-Gabrieli & Nieto-Castanon, 2012). The following steps were performed on the functional volumes: (1) slice-time (bottom-up, interleaved) and motion-correction, (2) skull-stripping and co-registration to the high-resolution structural image, (3) spatial normalisation to Montreal Neurological Institute (MNI)

space using the unified-segmentation algorithm, (4) smoothing with a 6mm FWHM Gaussian kernel, and (5) band-passed filtering (0.008-0.09Hz) to reduce low-frequency drift and noise effects. Nuisance regressors in the pre-processing pipeline included: (i) motion (12 parameters: the six translation and rotation parameters and their temporal derivatives), (ii) scrubbing (outliers were identified through the artefact detection algorithm included in CONN based on scan-by-scan change in global signal above z=3, subject motion threshold above 5mm, differential motion and composite motion exceeding 95% percentile in the normative sample), (iii) CompCor components (the first 5) attributable to the signal from white matter and CSF (Behzadi et al., 2007), and (iv) a linear detrending term, eliminating the need for global signal normalisation (Chai et al., 2012; Murphy et al., 2009).

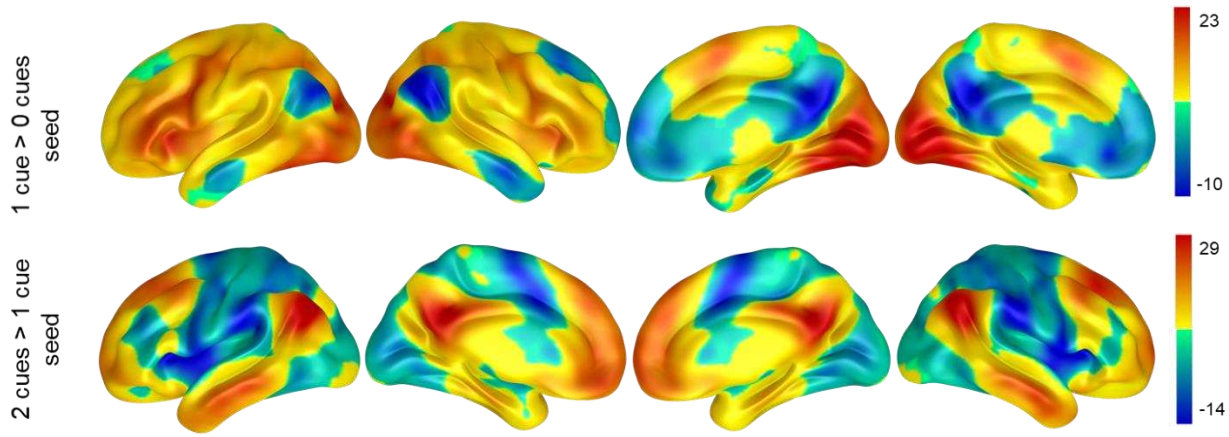

Figure S5. Intrinsic connectivity maps obtained in a separate sample of 86 participants using the thresholded (z > 3.1) contrast maps of 2 cues > 1cue and 1 cue > 0 as seeds in a resting state analysis. These reveal two functionally distinct and anti-correlated networks, comprising multiple demand regions for 1>0 and default mode regions for 2>1.